Level structure of the doubly-odd ^{242}Am nucleus

J.-L. Salicio, S. Drissi, M. Gasser, and J. Kern
Physics Department, University of Fribourg, CH-1700 Fribourg, Switzerland

H. G. Börner, G. G. Colvin, and K. Schreckenbach
Institut Laue-Langevin, 38042 Grenoble, France

R. W. Hoff and R. W. Lougheed
Lawrence Livermore National Laboratory, Livermore, California 94550
(Received 29 December 1987)

The level structure of the doubly-odd ^{242}Am nucleus was investigated by means of thermal-neutron-capture gamma-ray and conversion electron spectroscopy. Pair, curved-crystal, and β spectrometers were used. The data from these measurements, combined with previous direct reaction results, permit us to establish a detailed level scheme including six new well-developed bands. Our experimental results are interpreted in the framework of the Nilsson model. Precise Gallagher-Moszkowski splittings and Newby odd-even shifts extracted from the data are compared with theoretical calculations.

I. INTRODUCTION

Odd-odd nuclei provide interesting possibilities for studying the single particle structure and the proton-neutron residual interactions and consequently deserve a careful study. Boisson *et al.*[1] have reviewed the experimental results on deformed nuclei in the rare-earth region and made a theoretical analysis. In the actinide region only few isotopes have so far been carefully studied. A review of the available data can be found in Ref. 2. Additional precise experiments have to be performed to test current models and possibly disclose new effects in this heavier mass and strong deformation region.

Prior to our work, the following spectroscopic information was known on ^{242}Am: the ground state spin and parity[3] are $I^{\pi}=1^{-}$. An isomeric level lies at 48.6 keV excitation energy[4,5] and has spin and parity 5^{-}. This pair of levels forms the band heads of the $p\frac{5}{2}^{-}[523]\pm n\frac{5}{2}^{+}[622]$ Gallagher-Moszkowski doublet. About 68 levels had also been observed by direct ^{243}Am(d,t) and ^{241}Am(d,p) reactions.[6] Six rotational bands were thus identified.

In this paper we present results from a study of ^{242}Am by the reactions ^{241}Am(n,γ) and ^{241}Am(n,e^{-}). The spectra have been observed with high resolution spectrometers at the Eidgenössisches Institut für Reaktorforschung/Würenlingen (Switzerland) and the Institut Laue-Langevin (ILL)/Grenoble (France).

An account of the experimental methods and a presentation of the results will be given in Sec. II. We then discuss band by band in Sec. III the proposed level scheme. In addition to spectroscopic information, a simple semiempirical modeling technique[2,7] is used for configuration assignment. Conversely, our results test its predictive capability. In Sec. IV are presented the magnetic properties of the ground state band, a comparison between experimental and theoretical Gallagher-Moszkowski splittings and Newby shifts, and a statistical analysis of the level population.

II. EXPERIMENTAL METHODS AND RESULTS

A. High-energy (n,γ) spectrum

The 3.4 Ci ^{241}Am target (i.e., 1.1 g of Am_2O_3 powder) encapsuled—for reasons of safety—in a thin walled Al box, was irradiated at the Saphir reactor in Würenlingen (Switzerland) by an external thermal beam of neutrons having a flux of $\sim 2.5\times 10^{7}$ cm^{-2}s^{-1}. The γ rays following the reaction ^{241}Am(n,γ) were measured with the pair-spectrometer described in Ref. 8. A 20 cm^3 closed ended coaxial Ge(Li) detector was used. Its energy resolution was 3.6 keV FWHM at 4.7 MeV. The 59.5 keV line following the decay of ^{241}Am was suppressed by an absorber. The γ spectrum was observed in the energy range from $\sim$2 MeV to $\sim$6 MeV during $\sim$90 h. A portion of this spectrum is shown in Fig. 1. Impurity lines are mainly due to the reaction ^{27}Al(n,γ) on the target encapsulation. Other impurity lines are from radiative capture on Cl, N, H, I, Na, W, and possibly Fe, O, and C. The energies and intensities of the ^{27}Al(n,γ) transitions, which are precisely known,[9] were used to calibrate the ^{242}Am spectrum. The determination of the absolute intensities in number of photons per capture is based on estimations of the amount of Al used for the encapsulation and of the thermal neutron flux gradient across the target, and on the known capture cross sections[10] $\sigma_{Am}=624(21)b$ and $\sigma_{Al}=0.231(4)b$.

About 60 transitions have been attributed to ^{242}Am. Their energies and absolute intensities are presented in Table I. The given errors on the intensities are only statistical. Absolute errors are obtained by compounding them with an estimated 50% calibration error, which is

mainly due to the uncertainty on the effective amount of Al contributing in the $^{27}Al(n,\gamma)$ reaction.

With the hypothesis that the line at 5537.7(4) keV feeds the ground state, we obtain a good agreement between excitation energies deduced from the (n,γ) and transfer reaction results.[6] Using the energies of the primaries to the levels of the ground state band and to several other levels for which excitation energies are well established (see Sec. IV), we obtain a Q-value of 5537.7(1) keV for the $^{241}Am(n,\gamma)$ reaction. The recoil correction has been taken into account. The result differs slightly from the value obtained from the most recent mass evaluation,[11] i.e., 5539.4(5) keV.

B. Low-energy (n,γ) spectrum

The γ ray spectrum was measured with the DuMond spectrometers GAMS (Ref. 12) at the high-flux reactor of the ILL in Grenoble. The target was prepared at Oak Ridge National Laboratory and consisted of (0.4±0.1) mg of $^{241}AmO_2$ tightly wrapped in an aluminum holder, to a maximum total thickness of 0.5 mm. The neutron flux at the target was $\sim 5.5\times 10^{14}$ cm^{-2}s^{-1}.

With the 5.76 m DuMond spectrometer GAMS1, used in the energy range 30 keV $\leq E_\gamma \leq$ 400 keV, an angular resolution of 6–7 arcsec was obtained, corresponding to $\Delta E = 1.4\times 10^{-5} E_\gamma^2$ (keV)/n (n is the reflection order). In the spectrum there appears a very broad and intense bump at around 478 keV, which is characteristic of the $^{10}B(n,\alpha\gamma)^7Li$ reaction. The α particles are absorbed in the target material and holder, causing an additional heating above the usual temperature of 670 K. This produced a mechanical deformation of the target and resulted in a loss of resolution. For the energy calibration we used the 106.473(3) keV Am $K\alpha_1$ line.[13]

The 24 m twin-spectrometer GAMS2/3 used in the energy range 200 keV $\leq E_\gamma \leq$ 1200 keV had a resolution of 2 arcsec [$\Delta E = 3.7\times 10^{-6} E_\gamma^2$ (keV)/n]. The energy calibration was performed with the help of the strongest lines in the region 200 keV $\leq E_\gamma \leq$ 400 keV whose energies were already calibrated with GAMS1 measurement.

A special effort has been made to identify contaminant γ lines from fission products[14] which we simultaneously observed owing to the fission of ^{242}Am. The intensities were corrected for self-absorption in the target and for efficiency of the instruments.

A total of 317 transitions was observed. From this list, 108 were assigned to fission products, so that finally 209 lines were attributed to ^{242}Am. Their energies and intensities are listed in Table II. These results represent average values of data obtained with the two instruments and in general for several orders of reflection.

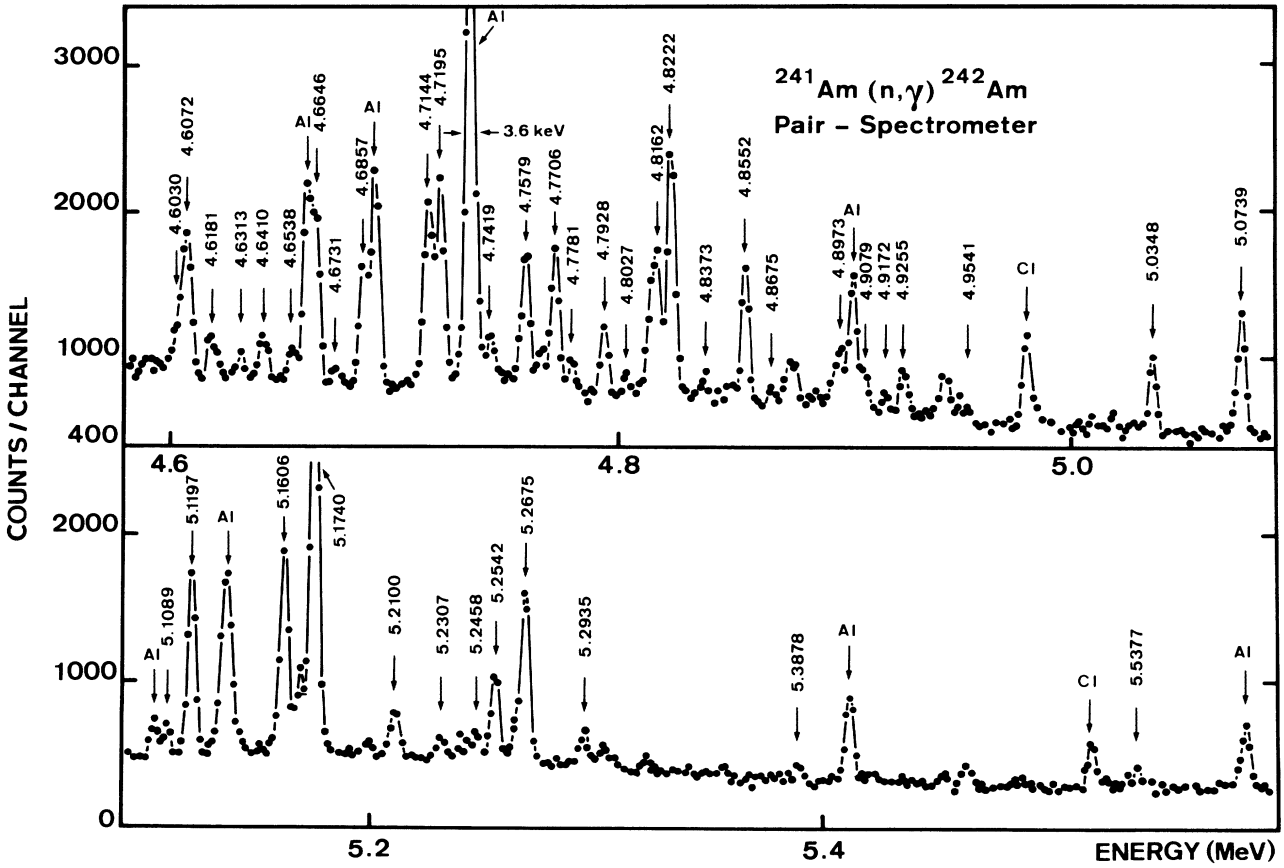

FIG. 1. Portion of the upper part of the $^{241}Am(n,\gamma)$ spectrum observed with the Fribourg pair spectrometer at the EIR/Würenlingen (Switzerland). The lines belonging to ^{242}Am are labeled by their energy in MeV.

TABLE I. High energy capture γ rays following the reaction ^{241}Am(n,γ)^{242}Am observed with a pair spectrometer (Ref. 8).

E_γ (keV)	ΔE_γ (keV)	I_γ ($\gamma/10^5$n)	ΔI_γ ($\gamma/10^5$n)	E (excited) $Q=5537.7\pm0.1$ keV
5537.7	0.4	4.3	0.7	0.0(4)
5485.2[a]	0.8	3.0	1.0	52.5(8)
5462.4[b]	0.3	2.5	1.0	75.3(8)
5387.8	0.4	3.2	0.6	149.9(4)
5340.0	0.7	1.5	0.5	197.7(7)
5306.4[c]	0.7	2.1	0.5	231.3(7)
5293.5	0.2	7.1	0.7	244.2(2)
5267.5	0.2	36.2	2.3	270.2(2)
5254.2	0.2	18.1	1.3	283.5(2)
5245.8[b]	0.3	2.8	1.0	291.9(3)
5230.7	0.4	4.0	0.6	307.0(4)
5210.0	0.3	9.1	0.9	327.7(3)
5174.0	0.2	92.0	5.4	363.7(2)
5167.3	0.3	14.4	1.2	370.4(3)
5160.6	0.3	42.3	2.6	377.1(3)
5137.4[c]	0.4	14.6	2.0	400.3(4)
5119.7	0.3	33.5	2.1	418.0(3)
5108.9	0.4	4.7	0.8	428.8(4)
5073.9	0.3	23.8	1.6	463.8(3)
5034.8	0.3	12.5	0.9	502.9(3)
5009.2	0.6	2.0	0.6	528.5(6)
4954.1	1.0	1.6	0.7	583.6(10)
4925.5	0.3	7.6	0.8	612.2(3)
4917.2	0.4	3.3	0.7	620.5(4)
4907.9	0.3	6.3	0.8	629.8(3)
4897.3	0.3	9.1	0.9	640.4(3)
4893.2	0.5	3.2	0.9	644.5(5)
4886.2	0.5	2.3	0.7	651.5(5)
4876.9 [d]	0.4	6.6	1.4	660.8(4)
4873.4 [d]	0.5	3.7	1.0	664.2(5)
4867.5	0.7	1.9	0.7	670.2(7)
4855.2	0.3	20.5	1.3	682.5(3)
4848.2[c]	0.5	2.5	0.7	689.5(5)
4837.3	0.5	2.8	0.9	700.4(5)
4822.2	0.3	28.4	2.1	715.5(3)
4816.2 [d]	0.3	19.0	1.8	721.5(3)
4813.1 [d]	0.3	11.1	1.9	724.6(3)
4802.7	0.5	2.6	0.8	735.0(5)
4792.8	0.5	10.3	1.1	744.9(5)
4778.1	0.4	4.1	0.9	759.6(4)
4770.6	0.3	18.0	1.3	767.1(3)
4757.9[b]	0.3	19.2	1.4	779.8(3)
4741.9	0.4	6.1	1.0	795.8(4)
4735.2[a,c]	0.4	20.4	3.9	802.5(4)
4719.5	0.3	29.7	1.7	818.2(3)
4714.4	0.3	24.1	1.6	823.3(3)
4685.7	0.3	16.3	1.2	852.0(3)
4673.1	0.7	2.0	0.8	864.7(7)
4664.6	0.3	22.5	1.5	873.1(3)
4653.8	0.4	4.9	1.0	883.9(4)
4641.0	0.3	5.8	0.7	896.7(3)
4631.3[a]	0.6	1.9	0.7	906.4(6)
4618.1[b]	0.4	3.2	0.7	919.6(4)
4607.2	0.3	18.1	1.1	930.5(3)
4603.0	0.4	5.0	0.9	934.7(4)

TABLE I. (*Continued*).

E_γ (keV)	ΔE_γ (keV)	I_γ ($\gamma/10^5$n)	ΔI_γ ($\gamma/10^5$n)	E (excited) $Q=5537.7\pm0.1$ keV
4568.9	0.3	11.1	0.9	968.8(3)
4562.7	0.5	5.0	1.1	975.0(5)
4559.3	0.3	22.5	2.0	978.4(3)

[a]Doubtful (weak).
[b]Result obtained after subtraction of a background line.
[c]Masked by an ^{28}Al line.
[d]Group of unresolved lines.

TABLE II. Low energy γ rays following the ^{241}Am(n,γ)^{242}Am reaction, observed with the GAMS spectrometers. I_γ is given in relative units. In column 3 are given the shells or subshells from which conversion electron groups were observed. The multipolarities are deduced from the conversion data.

$E_\gamma(\Delta E_\gamma)$ (keV)	$I_\gamma(\Delta I_\gamma)$	Shell observed	Multipolarity	Assignment E_i-E_f (keV)
30.973(1)	247(34)			419.1−388.2
32.195(2)[a]	163(26)	*M*2,*M*3		405.9−373.7
33.443(2)	151(27)	*M*1,*M*2	*E*1	405.9−372.5
33.713(2)	186(26)			
35.546(3)	107(22)	*M*1,*M*2,*M*3	(*M*1+*E*2)	
36.453(3)	86(17)	*L*3,*M*1,*M*3	(*M*1)	442.4−405.9
37.910(5)	90(21)	*L*3,*M*1,*M*2,*M*3		330.7−292.8
38.005(5)	54(18)	*M*1,*M*2,*M*3	*M*1(+*E*2)	
41.711(45)	20(2)	*L*1,*L*2,*L*3,*M*1		372.5−330.7
43.023(6)	36(15)	*M*2,*M*3	(*M*1+*E*2)	373.7−330.7
44.092(3)	113(16)	*L*1,*L*2,*L*3,*M*1,*M*2,*M*3	*M*1	44.1−0.0
48.514(30)	2(0.1)	*L*1,*L*2,*M*1,*M*2,*M*3		292.8−244.4
51.619(35)	2(1)	*L*1,*L*3,*M*1,*M*3	*M*1+*E*2	
52.770(36)	32(11)	*L*1,*L*2,*L*3,*M*1,*M*2,*M*3	*E*2	52.7−0.0
53.003(47)	81(15)	*L*1,*L*2,*M*1,*M*2	*M*1	1002.7−949.7
56.577(38)	13(5)	*L*2,*L*3,*M*2	*E*2	
57.236(28)	55(5)	*L*1,*L*2,*M*2,*M*3	*E*2(+*M*1)	
61.786(58)	620(9)	*L*1,*L*2,*L*3,*M*2,*M*3	*E*1	
62.876(15)	130(12)	*L*2,*L*3,*M*2	(*E*1)	355.7−292.8
65.408(28)	25(8)	*L*1,*L*2,*L*3,*M*1,*M*3		442.4−377.0
65.557(3)	103(11)	*L*1,*L*3,*M*2	(*E*1)	483.7−418.1
65.793(25)	840(76)	*L*1,*L*2,*L*3,*M*1,*M*2	*E*1	
67.439(4)	395(8)	*L*1,*L*3,*M*1,*M*2,*M*3	(*M*1+*E*2)	
68.701(3)[c]	175(12)			442.4−373.7
68.997(17)	32(9)	*L*1,*L*2,*L*3,*M*1,*M*2		457.2−388.2
69.101(8)	30(11)	*L*1,*L*2	(*E*1)	
69.253(11)	32(12)	*L*1,*L*3,*M*1	*M*1+*E*2	
69.448(11)	34(11)	*L*1,*L*3,*M*2,*M*3		
69.781(6)	46(15)	*L*1,*L*2,*L*3,*M*3	(*E*2)	400.5−330.7
71.593(7)	81(11)	*L*2,*L*3,*M*1		
75.664(7)	101(18)	*L*2,*L*3,*M*3		949.7−874.1
75.823(4)	543(11)	*L*1,*L*2,*L*3,*M*1,*M*2,*M*3	*M*1	75.8−0.0
76.092(14)	62(18)	*L*1,*L*2,*L*3,*M*2		372.5−296.4
76.258(13)	47(21)	*L*1		464.4−388.2
76.668(22)	32(15)	*L*1,*M*1		
77.988(23)	31(13)			405.9−327.9
78.945(19)	54(17)	*L*1,*L*2,*L*3,*M*2,*M*3		
80.400(33)	51(12)	*L*1,*L*2,*L*3,*M*1,*M*2	*M*1	
80.905(19)	40(12)	*L*1,*L*2,*L*3,*M*1,*M*2		373.7−292.8
81.312(15)	83(12)	*L*1,*L*2,*M*1,*M*2,*M*3		
81.864(32)	34(18)	*L*2,*M*1,*M*2,*M*3	*M*1+(14±6)%*E*2	
82.484(17)	67(16)	*L*1,*L*3,*M*1,*M*2,*M*3	*M*1+(16±10)%*E*2	
83.203(22)	53(18)	*L*1,*L*2,*L*3,*M*1,*M*2,*M*3	(*M*1+*E*2)	

TABLE II. (*Continued*).

$E_\gamma(\Delta E_\gamma)$ (keV)	$I_\gamma(\Delta I_\gamma)$	Shell observed	Multipolarity	Assignment $E_i - E_f$ (keV)
83.399(17)[c]	67(13)			457.2−373.7
83.926(12)	83(16)	*L*2,*L*3,*M*1	*M*1+*E*2	
84.124(2)	323(10)	*L*1,(*L*2,*L*3),*M*1,*M*2	(*E*1)	377.0−292.8
84.601(20)	65(20)			568.3−483.7
86.173(31)	87(32)	*L*1,*L*2,*M*1,*M*3	(*M*1+*E*2)	
86.316(30)	91(33)			330.7−244.4
86.487(11)	70(20)	*L*1,*L*3,*M*3	*E*1	
87.592(29)	55(35)	*L*1,*M*1		
87.726(31)	54(22)	*L*1,*L*2,*L*3,*M*1,*M*2	*M*1+*E*2	
88.322(31)	44(19)	*L*2,*L*3,*M*1,*M*2,*M*3	*M*1+(5±2)%*E*2	
88.869(19)	102(36)	*L*1,*L*3,*M*2,*M*3	*M*1+*E*2	
89.070(20)	112(32)	*L*2,*L*3,*M*2	*M*1+*E*2	
89.216(20)	125(20)	*L*1,*L*2,*L*3,*M*1,*M*3	*M*1+*E*2	
89.510(3)	1050(11)	*L*1,*L*3,*M*1,*M*2	*E*1	
89.799(24)	80(26)	*L*1,*L*3,*M*1,*M*2,*M*3	*M*1(+*E*2)	
90.178(22)	87(24)	*L*1,*M*1,*M*2		418.1−327.9
90.985(4)	118(11)	*L*1,*M*1		446.7−355.7
91.229(24)	55(17)	*L*2,*L*3,*M*1,*M*2,*M*3		419.1−327.9
92.568(26)	101(32)	*L*1,*L*2,*L*3,*M*2	*M*1+*E*2	
94.671(6)	113(11)	*L*1,*L*2,*L*3,*M*1,*M*2,*M*3	*M*1 + (18±7)%*E*2	244.4−149.7
94.804(5)	108(12)	*L*1,*L*2,*M*1,*M*3		364.7−269.9
94.874(22)	79(20)	*L*1,*L*3,*M*1,*M*3	*M*1+*E*2	
96.115(16)	129(26)	*L*2,*L*3,*M*1		1002.7−906.6
96.433(27)	76(27)	*L*1,*L*2,*L*3,*M*1		
96.994(2)	208(8)	*L*1,*L*2,*L*3,*M*1,*M*2	*M*1	149.7−52.7
98.161(5)	98(11)	*L*1,*L*2,*M*1,*M*2,*M*3	(*M*1+*E*2)	
100.352(43)	21(5)	*L*1,*L*2,*M*1,*M*2,*M*3	*M*1	
102.698(8)	84(15)	*L*2,*L*3,*M*1,*M*2,*M*3	(*E*1)	372.5−269.9
106.100(25)	325(49)	*L*1,*L*2,*L*3,*M*2	(*E*1)	
111.100(18)	86(12)	*L*1,*M*1	(*M*1)	341.6−230.5
111.274(47)	802(72)	*L*1,*L*2,*L*3,*M*2	*E*1	355.7−244.4
113.122(34)	95(12)	*L*1,*L*2,*L*3,*M*1,*M*2,*M*3	*M*1+*E*2	
113.699(11)	149(10)	*L*1,*L*3,*M*1,*M*2,*M*3	*M*1	
122.031(7)	134(16)	*L*1,*L*3,*M*1,*M*2,*M*3	*E*1	
124.755(22)	187(30)			
124.947(21)	121(29)	*L*2,*M*1	(*M*1)	
125.832(4)	1194(12)	*L*1,*L*2,*L*3,*M*1,*M*2,*M*3	*E*1	568.3−442.4
129.056(29)	62(21)	*L*1,*L*2		418.1−289.0
131.846(82)	113(18)	*L*1,*L*3,*M*1,*M*3	(*M*1+*E*2)	
132.565(4)	889(9)	*L*1,*L*2,*L*3,*M*1	*E*1	377.0−244.4
133.293(28)	74(23)	*L*1,*M*1,*M*3	*M*1+*E*2	
133.595(28)	77(18)			464.4−330.7
134.197(63)	68(20)	*L*1,*L*2,*L*3,*M*1	*M*1+*E*2	364.7−230.5
134.860(40)[a]	159(35)			
136.299(23)	35(13)	*L*2		
137.159(27)	45(9)	*L*1		
138.352(12)	79(8)	*L*1,*L*2	*E*2	
140.714(16)	64(10)			
142.306(25)	87(10)	*K*,*M*1	*E*2+(47±13)%*M*1	
143.789(28)	50(12)	*K*,*L*1,*L*2,*M*1		388.2−244.4
144.254(17)	79(10)	*L*1,*L*3		
144.890(29)	98(16)	*L*1,*L*2,*L*3		419.1−274.3
145.502(36)	73(9)	*K*,*L*1,*L*3,*M*1	*M*1+*E*2	
147.870(22)	77(9)	*K*,*L*1,*L*2,*L*3,*M*1,*M*3	*E*2+(40±10)%*M*1	(417.8−269.9)
148.386(37)	38(11)	*L*1,*L*3,*M*1,*M*3	(*M*1+*E*2)	612.8−464.4
149.713(11)	91(9)	*K*,*L*2	*M*1	
150.095(44)	131(22)	*K*,*L*2,*L*3		568.3−418.1
151.272(41)	103(19)			
154.708(2)	3595(29)	*L*1,*L*2,*L*3,*M*1,*M*3	*E*1	230.5−75.8
159.283(24)	206(10)	*K*,*L*2,*M*1,*M*2	*M*1	

TABLE II. (*Continued*).

$E_\gamma(\Delta E_\gamma)$ (keV)	$I_\gamma(\Delta I_\gamma)$	Shell observed	Multipolarity	Assignment $E_i - E_f$ (keV)
160.338(49)	43(15)	*K*,*L*3,*M*1,*M*3		
160.500(45)	17(5)	*K*,*L*1,*L*2,*M*1,*M*2	*E*2+(5±2)%*M*1	
161.459(18)	120(18)			405.9−244.4
163.933(44)	45(15)	*K*,*L*3,*M*2	*M*1 + (50±15)%*E*2	
165.079(41)	50(15)	*K*	*E*2 + (27±10)%*E*2	
165.786(56)	53(12)	*K*,*L*1,*L*2,*L*3,*M*1,*M*2	*M*1 + (40±10)%*E*2	
167.297(70)	110(21)			
168.125(30)	21(5)	*K*,*L*1	*E*1	457.2−289.0
168.519(8)	153(18)	*K*,*L*1,*L*2,*L*3,*M*1,*M*2	*M*1+*E*2	244.4−75.8
168.747(92)	115(30)	*K*	(*M*1+*E*2)	
171.951(25)	59(9)	*K*,*L*1,*M*1	(*M*1)	
173.599(157)	36(23)	*K*		418.1−244.4
175.314(34)	60(13)	*K*,*L*2,*M*1	*E*2 + (35±10)%*M*1	464.4−289.0
176.194(29)	68(12)	*K*,*L*1,*L*2	*M*1+*E*2	
176.972(45)	43(12)	*K*,*L*1,*L*2	*M*1+*E*2	
177.498(68)	104(22)	*K*	*E*2+(16±6)%*M*1	
178.110(67)	65(11)	*K*,*L*1,*L*3,*M*1	*M*1+*E*2	327.9−149.7
181.674(101)	76(24)	*K*,*L*1,*M*1,*M*2		
182.839(66)	33(15)	*K*,*L*2,*L*3,*M*1	*E*2	
183.476(43)	78(15)	*L*1,*L*2,*L*3,*M*2	*M*1 + *E*2	
185.143(179)	112(66)	*K*,*M*1,*M*2		
185.786(25)	102(21)	*K*,*L*1,*L*2,*M*2		
186.127(34)	196(74)	*L*1,*M*1,*M*2,*M*3	*M*1+*E*2	
186.433(2)	3277(31)	*K*,*L*1,*L*2,*M*1,*M*2,*M*3	*E*1	230.5−44.1
191.234(33)	1723(155)	*K*,*L*1,*L*2	*E*1	568.3−377.0
191.667(5)	606(7)	*K*,*L*1,*L*2,*M*1,*M*2	*M*1	244.4−52.7
192.108(6)	266(11)	*K*,*M*1	*M*1+*E*2	
193.128(31)	88(15)	*K*	*E*2	
193.677(23)	161(48)	*K*,*L*1,*L*2		612.8−419.1
194.510(5)	946(9)	*L*1,*L*2,*L*3	*E*1	464.4−269.9
195.778(6)	629(6)	*L*1,*L*2,*L*3,*M*1,*M*2,*M*3	*E*2	244.4−48.6
198.498(12)[c]	236(9)	*L*1,*L*2,*L*3,*M*1,*M*2	*M*1 + (45±11)%*E*2	274.3−75.8
199.291(20)	95(14)	*K*,*L*1,*M*1	*M*1	
201.982(63)	53(17)	*K*,*L*2,*L*3,*M*3	*E*2 + (20±10)%*M*1	
202.421(39)	69(17)	*K*,*L*1,*L*3	*E*2	
202.848(95)	62(12)	*K*	(*M*1+*E*2)	
212.536(14)	171(9)	*K*,*L*1	(*M*1+*E*2)	
213.370(80)[b]	239(86)	*K*,*L*1,*L*3,*M*1	*E*2	289.0−75.8
214.790(82)	44(17)	*K*,*L*1,*M*1	*M*1	
217.043(28)	111(10)	*K*,*L*1,*L*2,*M*1,*M*3	*M*1 + (50±7)%*E*2	292.8−75.8
218.429(36)	71(11)	*K*,*L*1,*L*2,*M*1	*M*1+*E*2	
220.600(24)	131(8)	*K*,*L*1,*L*2,*M*1	*M*1	296.4−75.8
222.751(86)	49(18)	*K*,*L*1,*L*2	*M*1+*E*2	372.5−149.7
224.902(81)	54(17)	*K*,*L*3	(*M*1+*E*2)	
225.408(44)	41(16)	*K*,*L*1,*L*2	*E*2 + (8±3)%*M*1	
230.242(7)	389(8)	*K*,*L*1,*L*2,*M*1,*M*2	*M*1	274.3−44.1
236.789(30)	94(9)	*K*,*L*1,*L*2,*M*1	*M*1	
240.115(14)	109(10)	*K*,*L*1,*M*1	*M*1 + (47±8)%*E*2	292.8−52.7
240.443(32)	130(17)	*K*	*E*2 + (34±8)%*M*1	289.0−48.6
243.690(11)	134(7)	*K*,*L*1,*L*2,*L*3,*M*1,*M*2	*M*1 + (23±14)%*E*2	296.4−52.7
252.049(15)	117(21)	*K*,*L*1,*L*2,*L*3,*M*1	*M*1+*E*2	327.9−75.8
254.840(16)	121(10)	*K*,*L*1,*L*2,*L*3,*M*1,*M*2	*M*1 + (28±9)%*E*2	330.7−75.8
255.467(38)	98(22)	*K*,*L*1,*L*3	*E*2	
256.007(33)	111(21)	*K*	(*M*1+*E*2)	
271.540(41)	100(14)	*K*,*L*1	*M*1+(*E*2)	
274.331(6)	986(10)	*K*,*L*1,*L*2	*M*1	274.3−0.0
275.087(16)	159(10)	*K*,*L*1,*L*2	*M*1+*E*2	327.9−52.7
278.000(18)	172(12)	*K*,*L*2		330.7−52.7
278.319(16)	199(12)	*K*,*L*1,*L*2,*L*3,*M*1	(*E*1)	

TABLE II. (*Continued*).

$E_\gamma(\Delta E_\gamma)$ (keV)	$I_\gamma(\Delta I_\gamma)$	Shell observed	Multipolarity	Assignment $E_i - E_f$ (keV)
293.341(61)	123(11)	*K*,*L*3	*E*2	
295.960(14)	223(9)	*L*1,*L*2,*L*3	*E*2	
296.412(25)	203(16)	*K*,*M*1,*M*2,*M*3	*M*1+*E*2	296.4−0.0
296.732(34)	115(13)	*K*,*L*1,*L*2,*L*3	(*E*2)	372.5−75.8
296.996(25)[c]	153(21)			446.7−149.7
302.766(25)	129(9)	*L*1,*L*3,*M*1	*E*2 + (41±11)%*M*1	
313.202(64)	87(20)	*K*,*L*1	*M*1+*E*2	
314.328(69)	105(17)	*K*,*L*1	*E*2(+*M*1)	
314.705(64)	86(20)	*K*,*L*1,*L*2,*L*3,*M*1	*M*1+*E*2	464.4−149.7
316.377(25)	140(14)	*K*,*L*1,*L*2	*M*1+*E*2	612.8−296.4
319.748(55)[b]	86(18)	*K*,*L*1*L*2	*M*1+*E*2	372.5−52.7
319.911(57)[b]	80(20)	*K*,*L*1,*L*2	*M*1+*E*2	612.8−292.8
324.844(57)	147(29)	*K*,*L*1,*M*1	*E*2 + (40±10)%*M*1	400.5−75.8
328.409(19)	151(11)	*K*,*L*1,*L*2	*M*1	
334.061(32)	81(18)	*L*1,*L*2	(*M*1)	483.7−149.7
341.528(22)[a]	123(14)	*K*,*L*2,*L*3		341.6−0.0
341.990(60)	125(24)	*L*1,*L*2,*L*3	*E*2	
343.948(32)	157(47)	*K*,*L*1,*L*2,*L*3	*E*1,*E*2	
350.294(139)	100(35)	*K*	*E*1	
352.396(16)	291(12)			
356.841(105)	144(37)	*K*	*E*1,*E*2	
361.357(11)	97(9)	*K*,*L*1,*L*2	*E*2	
366.351(33)	97(18)	*K*,*L*1,*L*2,*M*1	*M*1	419.1−52.7
368.237(62)	96(22)	*K*	*M*1+*E*2	612.8−244.4
368.875(65)	95(23)	*K*,*L*1	*E*2 + (10±4)%*M*1	
376.155(32)	180(45)	*K*,*L*2	*E*2	
382.234(30)	179(18)	*K*	*E*1,*E*2	612.8−230.5
384.531(27)	148(15)			
390.920(41)	126(16)			
397.955(25)	235(45)	*K*,*L*1	*E*2 + (40±10%)*M*1	
433.951(66)	75(18)	*K*	*E*1,*E*2	
435.038(22)[c]	324(14)			483.7−48.6
450.692(57)	102(21)	*K*,*L*1,*L*2	*M*1 + (40±10)%*E*2	
451.598(124)	79(21)	*K*,*L*1,*L*2	*E*2	
453.740(34)	97(21)	*K*,*L*1,*L*2	*M*1	
455.707(19)	318(22)	*K*	*E*1	
456.256(90)	260(49)	*K*	*E*1	
585.210(160)[c]	203(63)			874.1−289.0
586.723(154)	170(61)	*K*,*L*2	*E*2	
588.857(26)	313(19)	*K*	*E*1	
595.572(131)	169(61)	*K*,*L*1,*L*2	*E*2	
599.551(113)	171(61)	*K*,*L*1	*M*1+*E*2	
609.279(190)	111(21)			902.5−292.8
617.207(40)	101(10)	*K*,*L*1	*M*1	
629.640(73)	437(151)			874.1−244.4
658.106(59)	408(65)			902.5−244.4
691.916(96)	252(38)	*K*	*E*1	

[a]The conversion electrons lines are multiplets or lie in a complex region.
[b]Result of a complex γ-ray spectrum fit.
[c]Contaminated by a fission line, the fission intensity is subtracted.

C. The conversion electron spectrum

The ^{241}Am(n,e$^-$)^{242}Am spectrum was measured with the β spectrometer BILL (description and performance are given in Ref. 15) at the ILL. The target was prepared at Lawrence Livermore National Laboratory and consisted of a layer of ~0.4 mg Am_2O_3 produced by electrodeposition on a 1 mg/cm^2 Ni foil of 9×90 mm^2 and covered by a thin (20 μg/cm^2)Al layer. Electrons were counted with a multiwire proportional counter.[15] The momentum resolution was $\Delta p/p = 8\times10^{-4}$ at 200 keV. The energy calibration of the electron lines was per-

formed using the energies of a few well-defined transitions calibrated in the (n,γ) experiment. The intensities were corrected for absorption in the counter window and for the efficiency of the spectrometer.

The intensity normalization between the (n,e^-) and (n,γ) measurement was determined by adjusting absolute experimental to theoretical conversion coefficients[16] for transitions for which the multipolarity was determined from shell and subshell ratios. Selected results for transitions having a pure multipolarity are given in Table III. A portion of the electron spectrum is presented in Fig. 2 for illustration.

We report in Table II for each transition the list of shells and subshells from which we have observed electron groups. In some cases we observed electron conversion lines but not the corresponding γ-ray transitions in the GAMS spectra (Table IV). Various causes may be responsible for this situation, a region was masked by the broad 478 keV boron bump and a few regions of the γ spectrum were not scanned, for instance below 32 keV, due to time limitations. We have not listed in Table II the observed conversion coefficients and the corresponding theoretical values for the lowest multipolarities to avoid an excessively long table. These values are, however, available in the form of an unpublished report.[44]

III. CONSTRUCTION AND INTERPRETATION OF THE LEVEL SCHEME

The thermal neutron capture state has $I^\pi = 2^-$ and 3^-. Therefore, only low spin levels $(1 \leq I \leq 4)$ are expected to be populated by primary dipole transitions. To establish a precise level scheme, to identify the levels and their γ-decay, and to find their configuration assignments, we used the following information and methods.

(i) It was assumed that the spins and parity of the ground state band levels are correctly determined.

(ii) A number of levels are known from direct reaction experiments[6] (Table V). Furthermore, using the (n,γ) primary spectrum (Sec. II A), we determined the excitation energy of many levels with a precision of a few hundred eV.

(iii) The high precision of the low-energy transitions observed in this study permits the use of the Ritz combination principle. A level is more reliably established when it is connected by many transitions to other levels and when it corresponds to a level mentioned in (ii). A further test is given by the coherence of the observed multipolarities and of the decay pattern.

(iv) Depopulation of a level has to be higher than the observed population (intensity balance).

(v) Parameters for the observed rotational bands, band-head energies, and moments of inertia, are compared with predictions obtained from a model for excitations in odd-odd nuclei as described in Refs. 2 and 7. In using this model, we obtained the two-quasiparticle excitation energies and the rotational parameters from the experimental level structure of neighboring odd-A nuclei. Values for the Gallagher-Moszkowski splitting[17] and Newby odd-even shift[18] for any given band were obtained either from experimental data for the same configuration in another nearby odd-odd nucleus or from theoretical calculations (Ref. 2).

TABLE III. Conversion electron coefficients of some pure multipolarity transitions in ^{242}Am.

			Conversion coefficients[a]							
E_γ	I_γ	α[b]	K	$L1$	$L2$	$L3$	$M1$	$M2$	$M3$	Multipolarity
44.092	113	expt.		49.0(7)	8.6(1.2)	d	9.2(1.4)	1.6(3)	d	$M1$
		theor.		49.2	5.9	0.25	11.8	1.6	0.07	
75.823	543	expt.		11.7(4)	1.3(1)	0.05(1)	2.5(1)	0.30(1)	d	$M1$
		theor.		10.0	1.2	0.05	2.4	0.33	0.01	
80.400	51	expt.		9.0(2.1)	1.1(3)		d	0.3(1)		$M1$
		theor.		8.4	1.0	0.04	2.0	0.3	0.01	
89.510	113	expt.		d	c	4.2(5)	1.5(3)	0.8(1)	d	$E1$
		theor.		5.9	4.2	3.6	1.4	1.0	0.9	
96.994	208	expt.		4.5(2)	0.46(4)	d	1.1(1)	0.12(1)		$M1$
		theor.		4.9	0.61	0.02	1.2	0.16	0.01	
125.822	1194	expt.		2.9(1)	2.4(1)	1.3(1)	0.67(5)	d	d	$E1$
		theor.		2.9	1.6	1.2	0.67	0.38	0.31	
132.565	889	expt.		2.7(1)	1.5(2)	1.3(1)	0.85(9)	d	d	$E1$
		theor.		2.6	1.4	1.1	0.60	0.33	0.27	
186.433	3277	expt.	9.3(5)	1.26(3)	0.76(3)	d	0.36(4)	d	0.12(2)	$E1$
		theor.	9.6	1.24	0.52	0.36	0.29	0.13	0.09	
220.600	131	expt.	2.59(16)	0.48(3)	0.07(1)		0.10(1)			$M1$
		theor.	2.59	0.46	0.06	0.002	0.11	0.01	0.0006	

[a]For $E1$ transitions the α values must be multiplied by a factor of 10^{-2}.

[b]The theoretical conversion coefficients are taken from Hager and Seltzer (Ref. 16).

[c]Masked by a strong conversion line due to another transition.

[d]Multiplet structure.

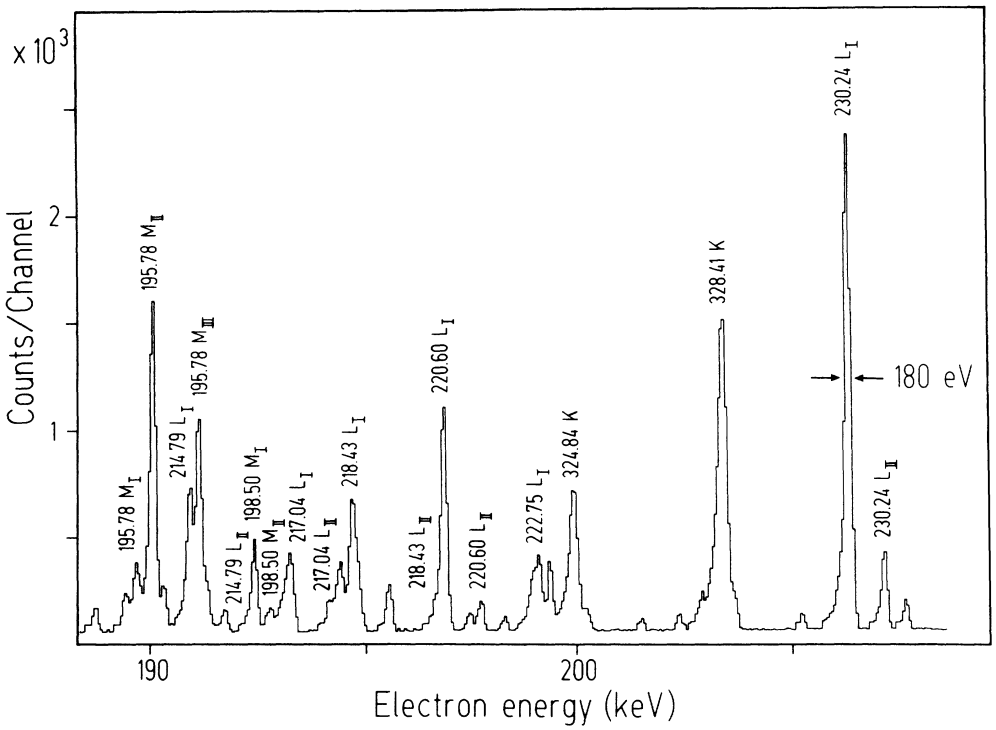

FIG. 2. Part of the conversion spectrum observed with the β spectrometer (BILL) at the ILL/Grenoble (France).

In order to distinguish model independent and model dependent spin assignments, we have listed in Table V both the level spins and parities deduced from the observed transition multipolarities and the adopted values. We have assumed that all not too weak primaries have dipole character.

The level scheme resulting from our study is presented in Figs. 3–7. A total of 12 rotational bands were established; six of these had not been previously observed. To shorten the notation we have assigned a unique letter to each particle orbital (see Fig. 3). These letters are also given, together with information on the relative intrinsic spin orientation, in the headings of the following sections.

A. The $K^\pi=0^-\{p\frac{5}{2}^-[523]-n\frac{5}{2}^+[622]\}$ band ($AZ\uparrow\downarrow$)

The ground state spin and parity have been determined[3] to be 1^-. Asaro *et al.*[4] suggested that this state is the lowest member of the $\{p\frac{5}{2}^-[523]-n\frac{5}{2}^+[622]\}$ $K=0$ rotational band. The K quantum number was deduced from a study of β-ray branching ratios and from the quadrupole and magnetic moments of this level. The suggested orbitals form the ground state in the neighboring isotopes ^{241,243}Am and isotones ^{241}Pu and ^{243}Cm (data of Refs. 19 and 20). The appearance of the $I=1$ spin level as the lower energy member of the band is due to a positive Newby odd-even shift.[18] Four excited levels at 50 keV ($0^-,3^-$), 76 keV (2^-), 148 keV ($4^-,5^-$), and 263 keV ($6^-,7^-$) had been observed by direct reaction spectroscopy.[6] We observe the depopulation of the four excited states with spin 0^-, 2^-, 3^-, and 4^- (Fig. 3).

Using the observed band structure, we analyzed the $K=0$ rotational band in terms of the well-known formula

$$E(I)=E_0+AI(I+1)-(-1)^I E_N\pi\ , \qquad (1)$$

where π denotes the parity of the states[1] [$\pi=+1(-1)$ for positive (negative) parity, respectively] and E_N is the Newby shift. The obtained value $A=5.28(11)$ keV is consistent with the predicted one (Table VI). The value of E_N, 27.3 keV, will be discussed in Sec. IV B.

B. The $K^\pi=5^-\{p\frac{5}{2}^-[523]+n\frac{5}{2}^+[622]\}$ isomeric band ($AZ\uparrow\uparrow$)

The $K^\pi=5^-\{p\frac{5}{2}^-[523]+n\frac{5}{2}^+[622]\}$ band is built on the $T_{1/2}=141$ yr isomeric level at 48.62 keV which is known[4,5] to be the band head. Two excited states at 114 and 190 keV have been identified in the direct neutron transfer reactions (Fig. 3). Only the band head is populated in the present experiments.

The rotational parameter, $\hbar^2/2\Theta=5.44(11)$ keV, is very similar to that observed for the ground state band (see Table VI). The Gallagher-Moszkowski splitting,[17] 5.3(7) keV, will be discussed in Sec. IV B.

C. The $K^\pi=0^+\{p\frac{5}{2}^+[642]-n\frac{5}{2}^+[622]\}$ band ($BZ\uparrow\downarrow$)

The energies of the two most intense transitions in the low-energy (n,γ) spectrum are 154.708 and 186.433 keV. They depopulate a level at 230.53 keV (Fig. 3), which is populated by the 5306.4 keV primary (Table I). The $E1$ multipolarity of the 154.708 and 186.433 keV γ rays determines the level spin and parity to be $I^\pi=1^+$.

The lowest positive parity band is expected to have the configuration $\{p\frac{5}{2}^+[642]-n\frac{5}{2}^+[622]\}K^\pi=0^+$. If this band has a negative Newby shift, as expected theoretical-

ly (see Table VIII), the band head should be the 1^+ state. The assumption that the 230.5 keV level has $I^\pi K = 1^+0$ is supported by application of the Alaga[21] rule (see Table VII).

Since the proton orbital is not the same as in the ground state of the target nucleus, the levels of the $\{p\frac{5}{2}^+[642]-n\frac{5}{2}^+[622]\}$ band are not expected to be populated in the (d,t) reaction. This holds for the 230.5 keV level. By application of the Ritz principle and by use of the modeling technique, further band members were found at 269.9(3^+), 341.6(0^+), 364.7(2^+), and possibly 417.8(4^+) keV. None of them is seen in the (d,t) experiment, as expected. Three of them (2^+, 3^+, and 4^+) are populated by intense primaries, of probable $E1$ multipolarity, confirming the positive parity of the final levels. The rotational parameter, 4.1 keV, is slightly larger than predicted (cf. Table VI). The experimental band head energy, 230.5 keV, is in good agreement with the predicted one [211(63) keV, see Table VI]. The Newby shift of the band is $-59.4(4)$ keV (see discussion in Sec. IV B).

D. The $K^\pi = 3^-\{p\frac{5}{2}^-[523]+n\frac{1}{2}^+[631]\}$ band ($AY\uparrow\uparrow$)

Levels of this band up to spin 7^- have been previously identified.[6] We observe the $I^\pi = 3^-$ band head at 244.4 keV. A $I^\pi = 4^-$ band member at 289.01 keV is identified by three decay transitions. The excitation energy is in accordance with the value (290 keV) observed in the (d,p) and (d,t) measurements.[6] The rotational parameter, 5.57(10) keV, agrees well with the predicted value (Table

TABLE IV. Transitions observed in the (n,e$^-$) experiment only. The transition energies are computed from the conversion electron measurements by adding the proper binding energies. The multipolarities were determined from subshell ratios.

$E_\gamma(\Delta E_\gamma)$ (keV)	Computed I_γ[a]	Shell observed	Multipolarity	Assignment $E_i - E_f$ (keV)
23.123(70)	0.2	*M*2,*M*3	*E*2	364.7 – 341.6
25.124(51)	0.1	*M*1,*M*2,*M*3	*E*2	
26.922(54)		*M*1,*M*2,*M*3		
27.820(57)	322.0	*M*1,*M*2	*E*1	355.7 – 327.9
28.937(25)		*M*1,*M*2,*M*3		405.9 – 377.0
29.351(19)	30.0	*M*1,*M*2,*M*3	*M*1	
29.937(53)		*M*1,*M*2,*M*3		418.1 – 388.2
31.306(36)	~0.2	*M*1,*M*2,*M*3	*M*1 + (90%)*E*2	
32.526(21)	~1.0	*M*1,*M*2,*M*3	*M*1 + (10%)*E*2	906.6 – 874.1
33.803(47)	0.6	*M*1,*M*2,*M*3	*E*2	
34.441(13)	0.8	*M*1,*M*2	*M*1	330.7 – 296.4
35.049(11)		*M*1,*M*2,*M*3		327.9 – 292.8
35.842(75)		*M*1,*M*2,*M*3		400.5 – 364.7
38.145(10)		*M*1,*M*3		
38.996(9)	~3.8	*M*1,*M*2,*M*3	*M*1 + (20%)*E*2	457.2 – 418.1
39.415(63)	0.1	*L*3,*M*2,*M*3	(*E*2)	269.9 – 230.5
41.997(34)	5.0	*M*1,*M*2,*M*3	*E*2	
43.172(45)	~15.0	*L*1,*L*2,*M*1,*M*2,*M*3	*M*1 + (5%)*E*2	949.7 – 906.6
43.728(23)	6.0	*L*2,*L*3,*M*1	*M*1	
44.557(25)	~6.4	*L*1,*L*2,*L*3,*M*1,*M*2,*M*3	*M*1 + (13%)*E*2	289.0 – 244.4
45.912(61)	~9.3	*L*2,*L*3	*M*1 + (2%)*E*2	373.7 – 327.9
46.128(33)		*L*1,*L*2,*L*3		446.7 – 400.5
46.419(44)		*M*2,*M*3		
46.598(16)	0.55	*L*1,*L*2,*L*3,*M*2,*M*3	(*E*2)	419.1 – 372.5
49.026(46)		*L*1,*L*2,*L*3,*M*3		377.0 – 327.9
50.268(42)	0.1	*L*2,*L*3,*M*2,*M*3	(*E*2)	405.9 – 355.7
52.045(69)	1.0	*L*1,*L*2	*M*1	296.4 – 244.4
56.421(18)		*L*2,*M*2,*M*3		330.7 – 274.3
59.249(37)	7.9	*L*1,*L*2,*L*3	*E*2	
64.541(31)		*L*1,*L*2,*L*3,*M*3		483.7 – 419.1
72.806(30)	1.1	*L*2,*L*3,*M*3	(*E*2)	400.6 – 327.9
73.864(11)	2.0	*L*2,*L*3,*M*3	*E*2	149.7 – 75.8
74.248(23)	5.3	*L*1,*L*2,*M*1	*M*1	446.7 – 372.5
88.438(50)	~7.0	*L*1,*L*2,*M*1	*M*1 + (60%)*E*2	419.1 – 330.7
95.440(60)	190.0	*L*1,*L*3,*M*1,*M*2	*E*1	388.2 – 292.8
99.269(15)[b]	510.0	*L*1,*M*1,*M*2	*E*1	388.2 – 289.0

[a]For mixed multipolarity transitions, we have assumed mixing ratios (in parentheses in column 4) which give the best agreement between the computed γ-ray intensities. Since many lines include more than one component, the proposed values have, in general, a considerable uncertainty.

[b]Masked by a Pu-x-ray line.

TABLE V. Assigned levels in ^{242}Am.

Level energy from secondary γ rays (keV)	I^{π} expt.[a]	$I^{\pi}K$ adopted	Level energy from primary γ rays (keV)	Energy from (d,p),(d,t)[b] (keV)	Proposed Nilsson configuration
0.0		1^-0	0.0	0	$\frac{5}{2}^-[523]-\frac{5}{2}^+[622]$
44.093(5)	0^-	0^-0		44	$\frac{5}{2}^-[523]-\frac{5}{2}^+[622]$
48.622(30)	5^-	5^-5		49	$\frac{5}{2}^-[523]+\frac{5}{2}^+[622]$
52.735(20)	3^-	3^-0	52.5(8)	49	$\frac{5}{2}^-[523]-\frac{5}{2}^+[622]$
75.820(10)	2^-	2^-0	75.2(3)	75	$\frac{5}{2}^-[523]-\frac{5}{2}^+[622]$
		6^-5		114	$\frac{5}{2}^-[523]+\frac{5}{2}^+[622]$
		5^-0		148	$\frac{5}{2}^-[523]-\frac{5}{2}^+[622]$
149.728(35)	4^-	4^-0	149.9(4)	148	$\frac{5}{2}^-[523]-\frac{5}{2}^+[622]$
		7^-5		190	$\frac{5}{2}^-[523]+\frac{5}{2}^+[622]$
230.526(10)	1^+	1^+0	231.3(7)		$\frac{5}{2}^+[642]-\frac{5}{2}^+[622]$
244.401(35)	3^-	3^-3	244.2(2)	245	$\frac{5}{2}^-[523]+\frac{1}{2}^+[631]$
		$6^-,7^-0$		263	$\frac{5}{2}^-[523]-\frac{5}{2}^+[622]$
269.862(50)	$2^+,3^+$	3^+0	270.2(2)		$\frac{5}{2}^+[642]-\frac{5}{2}^+[622]$
274.329(10)	1^-	1^-1			$\frac{5}{2}^-[523]-\frac{7}{2}^+[624]$
289.010(55)	4^-	4^-3		288	$\frac{5}{2}^-[523]+\frac{1}{2}^+[631]$
292.836(15)	$2^-,3^-$	2^-2	291.9(3)	288	$\frac{5}{2}^-[523]-\frac{1}{2}^+[631]$
296.420(15)	2^-	2^-1			$\frac{5}{2}^-[523]-\frac{7}{2}^+[624]$
327.868(35)	3^-	3^-2	327.7(3)	325	$\frac{5}{2}^-[523]-\frac{1}{2}^+[631]$
330.741(30)	3^-	3^-1			$\frac{5}{2}^-[523]-\frac{7}{2}^+[624]$
		5^-3		341	$\frac{5}{2}^-[523]+\frac{1}{2}^+[631]$
341.588(45)	$(0^+,1^+,2^+)$	0^+0			$\frac{5}{2}^+[642]-\frac{5}{2}^+[622]$
355.714(25)	$2^+,3^+(4^+)$	2^+2			$\frac{5}{2}^+[642]-\frac{1}{2}^+[631]$
364.718(20)	$1^+,2^+$	2^+0	363.7(2)		$\frac{5}{2}^+[642]-\frac{5}{2}^+[622]$
372.506(15)	$3^-,4^-$	4^-1	370.4(3)		$\frac{5}{2}^-[523]-\frac{7}{2}^+[624]$
373.746(20)	$2^-,3^-,4^-$	4^-2		372	$\frac{5}{2}^-[523]-\frac{1}{2}^+[631]$
376.962(25)	$2^+,3^+$	3^+2	377.1(3)		$\frac{5}{2}^+[642]-\frac{1}{2}^+[631]$
388.166(30)	$3^+,4^+$	3^+3			$\frac{5}{2}^+[642]+\frac{1}{2}^+[631]$
400.532(60)	$1^-,2^-,3^-$	1^-1	400.3(4)		$\frac{3}{2}^-[521]-\frac{5}{2}^+[622]$
405.949(35)	$2^+,3^+,4^+$	4^+2			$\frac{5}{2}^+[642]-\frac{1}{2}^+[631]$
		6^-3		410	$\frac{5}{2}^-[523]+\frac{1}{2}^+[631]$
417.800(50)	$1^+,2^+,3^+,4^+$	4^+0	418.0(3)		$\frac{5}{2}^+[642]-\frac{5}{2}^+[622]$
418.120(20)	$2^+,3^+,4^+$	4^+3			$\frac{5}{2}^+[642]+\frac{1}{2}^+[631]$
419.139(25)	$2^-,3^-,4^-$	2^-1			$\frac{3}{2}^-[521]-\frac{5}{2}^+[622]$
		5^-2		430	$\frac{5}{2}^-[523]-\frac{1}{2}^+[631]$
442.424(25)	$3^+,4^+,5^+$	5^+2			$\frac{5}{2}^+[642]-\frac{1}{2}^+[631]$
446.700(20)	3^-	3^-1			$\frac{3}{2}^-[521]-\frac{5}{2}^+[622]$
457.158(25)	$3^+,4^+,5^+$	5^+3			$\frac{5}{2}^+[642]+\frac{1}{2}^+[631]$
464.371(30)	$3^-,4^-$		463.8(3)		
483.677(45)	$3^-,4^-,5^-$	4^-1			$\frac{3}{2}^-[521]-\frac{5}{2}^+[622]$
		7^-3		488	$\frac{5}{2}^-[523]+\frac{1}{2}^+[631]$
		6^-2		500	$\frac{5}{2}^-[523]-\frac{1}{2}^+[631]$
568.256(25)	$3^-,4^-$				
		7^-2		581	$\frac{5}{2}^-[523]-\frac{1}{2}^+[631]$
612.782(35)	$2^-,(3^-)$		612.2(3)	(608)	
		8^-2		679	$\frac{5}{2}^-[523]-\frac{1}{2}^+[631]$
874.072(70)	$2^-,3^{\pm},4^-$	2^-2	873.1(3)	873	$\frac{5}{2}^-[523]-\frac{1}{2}^+[620]$
902.47(12)	$1^-,2^{\pm},3^{\pm},4^{\pm},5^-$	3^-3		899	$\frac{5}{2}^-[523]+\frac{1}{2}^+[620]$
906.59(8)	$1^{\pm},2^{\pm},3^{\pm},4^{\pm}$	3^-2	906.4(6)		$\frac{5}{2}^-[523]-\frac{1}{2}^+[620]$
949.74(8)	$0^{\pm},1^{\pm},2^{\pm},3^{\pm},4^{\pm},5^{\pm}$	4^-2		951	$\frac{5}{2}^-[523]-\frac{1}{2}^+[620]$
		3^+3	975.0(5)	975	$\frac{5}{2}^-[523]+\frac{1}{2}^-[501]$
1002.71(9)	$0^{\pm},1^{\pm},2^{\pm},3^{\pm},4^{\pm},5^{\pm}$	5^-2			$\frac{5}{2}^-[523]-\frac{1}{2}^+[620]$
		2^+2		1011	$\frac{5}{2}^-[523]-\frac{1}{2}^-[501]$

TABLE V. (*Continued*).

Level energy from secondary γ rays (keV)	I^{π} expt.[a]	$I^{\pi}K$ adopted	Level energy from primary γ rays (keV)	Energy from (d,p),(d,t)[b] (keV)	Proposed Nilsson configuration
		4^+3		1031	$\frac{5}{2}^-[523]+\frac{1}{2}^-[501]$
		3^+2		1051	$\frac{5}{2}^-[523]-\frac{1}{2}^-[501]$
		5^+3		1065	$\frac{5}{2}^-[523]+\frac{1}{2}^-[501]$
		4^+2		1098	$\frac{5}{2}^-[523]-\frac{1}{2}^-[501]$

[a]Deduced from the multipolarities of the observed transitions.
[b]Taken from Ref. 6.

VI). The predicted band head energy (169 keV) is somewhat smaller than the observed one.

It is seen (Fig. 3) that the observed levels decay to those of the $\{p\frac{5}{2}^-[523]\pm n\frac{5}{2}^+[622]\}$ bands. The sole unpaired neutron changes its configuration, and this with f-forbiddeness $\Delta\Omega_n=2$. We note that transitions between $n\frac{1}{2}^+[631]$ and $n\frac{5}{2}^+[622]$ states are also observed in the neighboring odd-N Pu and Cm isotones.[19,20,22,23] The same feature is also observed[24] in ^{244}Am.

E. The $K^{\pi}=1^-\{p\frac{5}{2}^-[523]-n\frac{7}{2}^+[624]\}$ band ($AX\uparrow\downarrow$)

This band is developed up to spin 4 by application of the Ritz principle. The results are also supported by intensity balance considerations. The configuration assignment of this band is justified by the following considerations.

(i) The band head spin and parity are uniquely determined to be $I^{\pi}=1^-$ by the $M1$ multipolarity of the 230.24

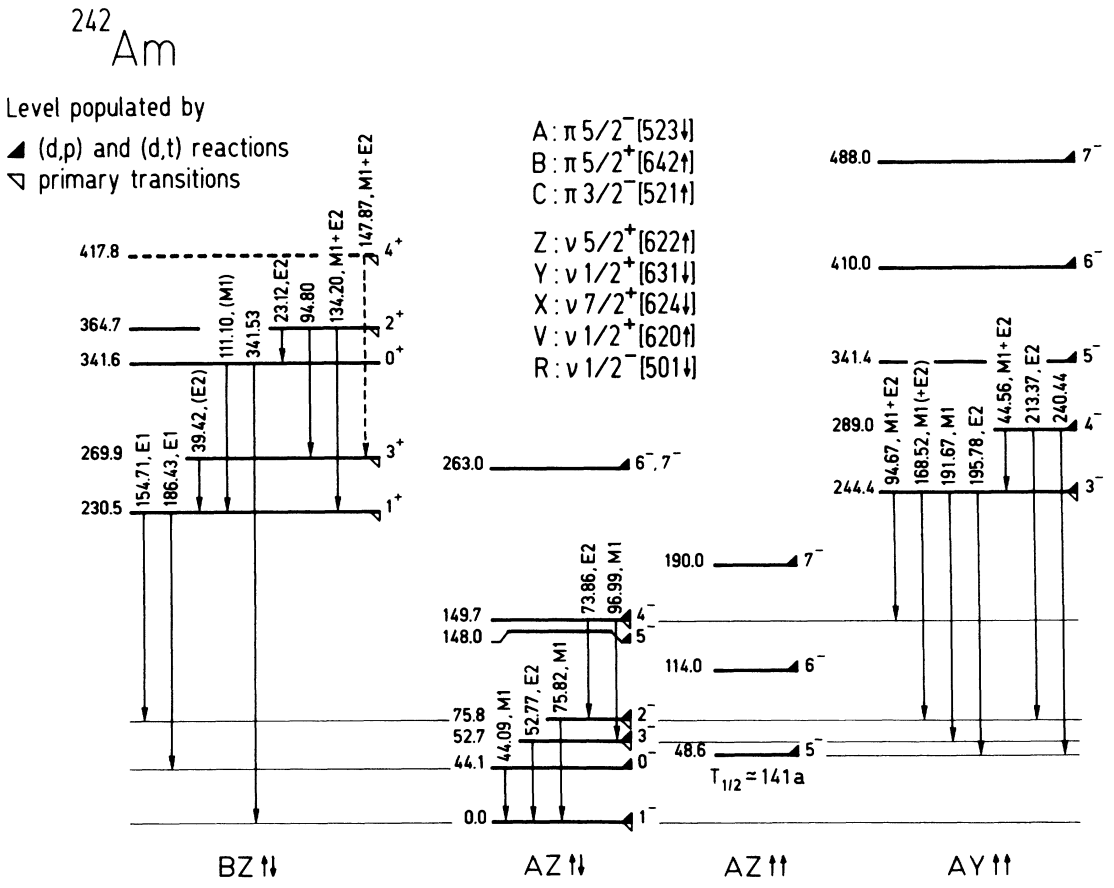

FIG. 3. Part 1 of the ^{242}Am level scheme. Levels observed in the transfer reaction measurements (by primary transitions) are indicated with ◢ (◥).

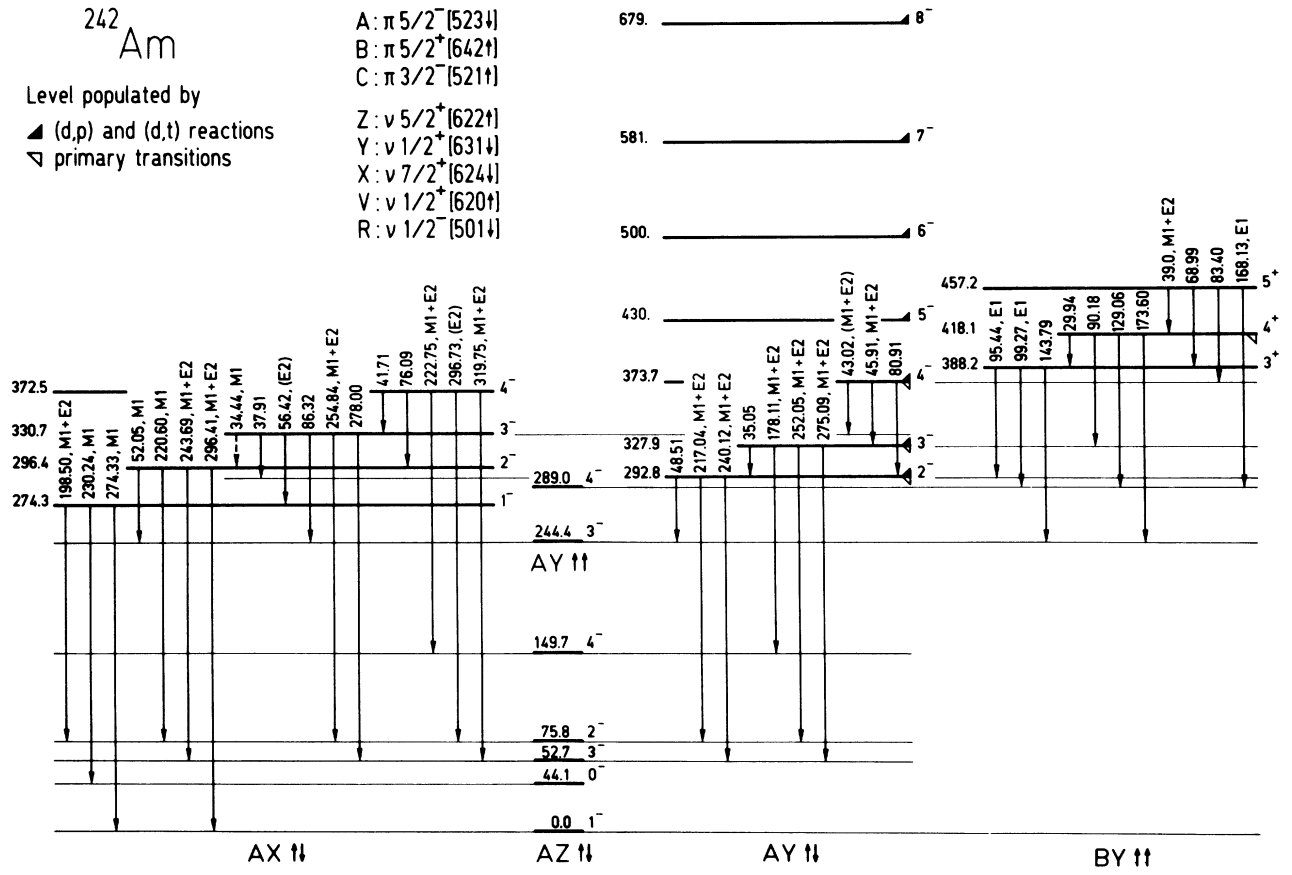

FIG. 4. Part 2 of the ^{242}Am level scheme (same caption as for Fig. 3).

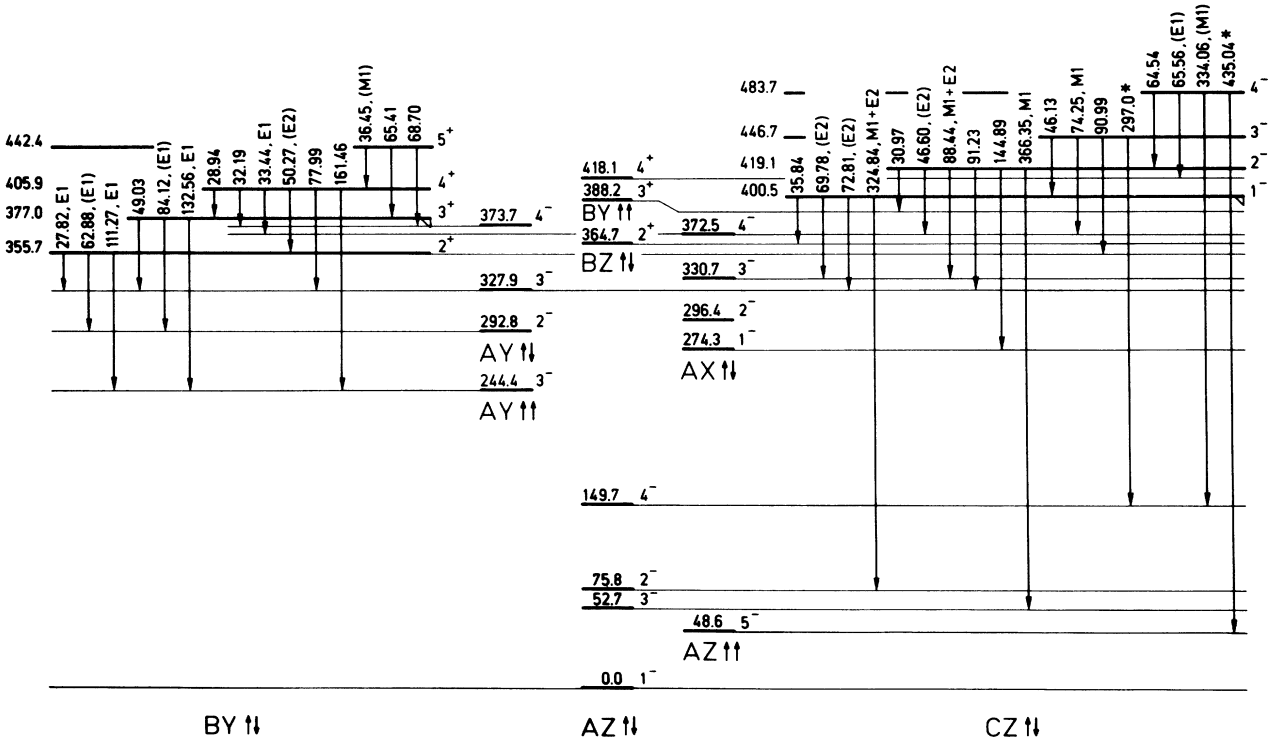

FIG. 5. Part 3 of the ^{242}Am level scheme (same caption as for Fig. 3).

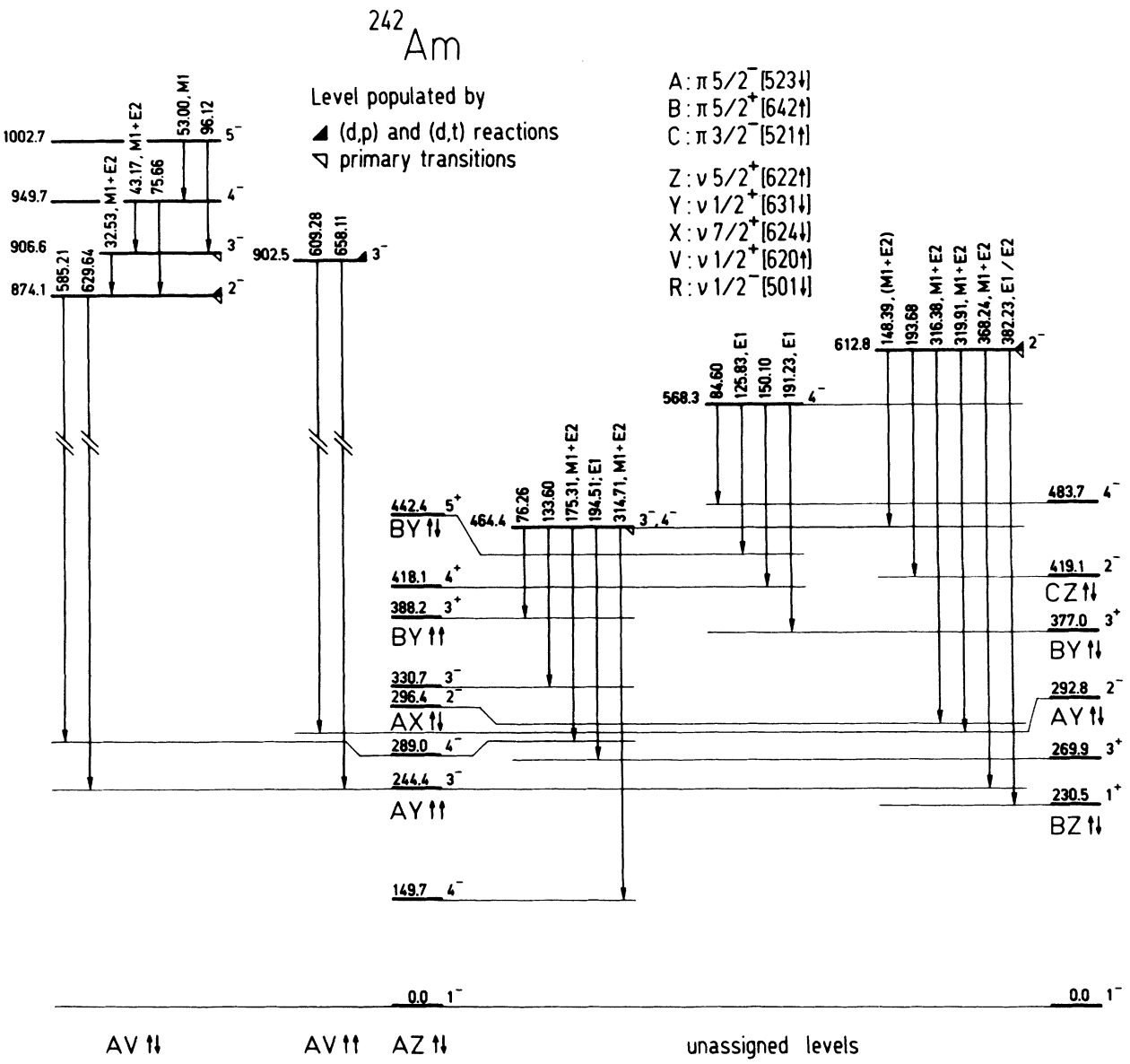

FIG. 6. Part 4 of the ^{242}Am level scheme (same caption as for Fig. 3).

and 274.33 keV transitions.

(ii) The spin and parity of the 296.4 keV level are uniquely determined to be $I^{\pi}=2^{-}$ from the multipolarities of the depopulating transitions.

(iii) The band head is predicted at 288(53) keV with a rotational parameter of 5.3(3) keV, in agreement with the experimental values [274.3 keV and 5.7(1) keV, respectively].

(iv) The band depopulates by transitions to final levels where the proton is in the $p\frac{5}{2}^{-}[523]$ orbital which should also be present in the initial levels.

(v) The Alaga rule is very well satisfied for $K_i=1$ (Table VII).

(vi) The same band is also observed[24] in ^{244}Am with a similar rotational parameter.

The band is not populated in the charged particle reactions.[6] This is because of the smallness of the cross section to the $n\frac{7}{2}^{+}[624]$ orbital, which is about ten times lower than the $n\frac{5}{2}^{+}[622]$ orbital (see, e.g., Ref. 25).

F. The $K^{\pi}=2^{-}\{p\frac{5}{2}^{-}[523]-n\frac{1}{2}^{+}[631]\}$ band ($AY\uparrow\downarrow$)

Seven band members were observed by Grotdal *et al.*,[6] including the band head at 290 keV. Combining the results from our (n,γ) experiments, we have identified the $I^{\pi}=2^{-}$, 3^{-}, and 4^{-} levels at 292.8, 327.9, and 373.7 keV, respectively. The excitation energy of the 2^{-} level differs slightly from the one obtained from the transfer reaction results.[6] This is due to the unresolved doublet structure of the charged particle groups[6] leading to levels at about 288 keV. The experimental band head energy and rotational parameter agree with the predictions (Table VI).

It can be noted that a moderately intense primary populates a level at 428.8 keV (Table I). This level has not been identified as the 430 keV level observed in the

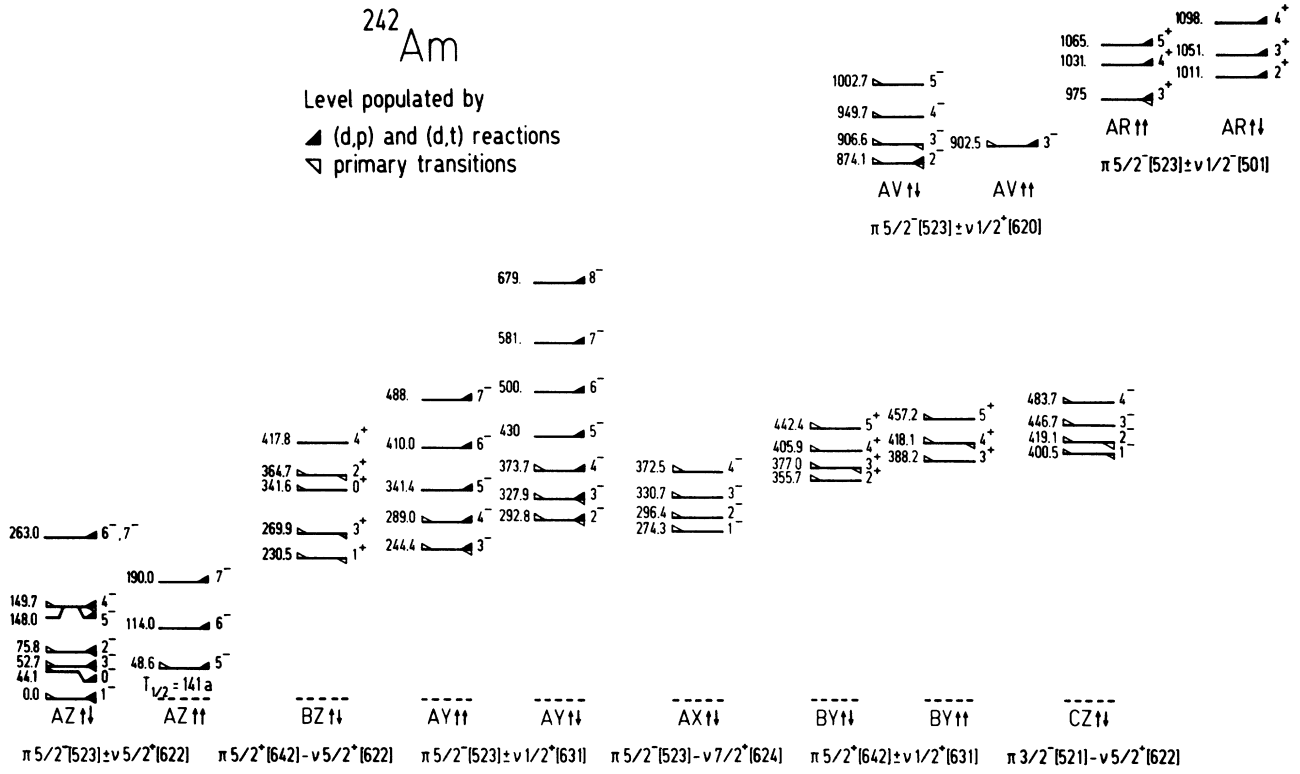

FIG. 7. Summary of assigned levels in ^{242}Am observed in this and in previous studies.

transfer experiment[6] (see Table V), since it would imply an $E2$ multipolarity for the primary. This does not seem in agreement with its observed intensity.

Inspection of Table VI shows that there is a small difference between the experimental rotational parameter of the $K^\pi=3^-$ and $2^-\{p\frac{5}{2}^-[523]\pm n\frac{1}{2}^+[631]\}$ bands. This can be explained by Coriolis interaction. Bohr and Mottelson[26] give the following relation for the rotational parameter difference in this case:

$$A(K_>)-A(K_<)=2Aa^2/[E(K_>)-E(K_<)]\ , \quad (2)$$

where $K_>=\Omega_p+\frac{1}{2}$, $K_<=\Omega_p-\frac{1}{2}$, A represents the aver-

TABLE VI. Comparison between experimental and predicted band head energies and rotational parameter for some bands of ^{242}Am.

Configuration			Band head energy (keV)		Rotational parameter (keV)	
π	ν	K^π	$E_{pred.}$	$E_{expt.}$	$A_{pred.}$	$A_{expt.}$
$\frac{5}{2}^-[523]$	$\frac{5}{2}^+[622]$	0^-	0	0.0	5.1(4)	5.28(11)
		5^-	112(40)	48.6	5.1(4)	5.44(11)
$\frac{5}{2}^-[523]$	$\frac{7}{2}^+[624]$	6^-	126(20)	5.3(3)	5.3(3)	
		1^-	288(53)	274.3	5.3(3)	5.7(1)
$\frac{5}{2}^-[523]$	$\frac{1}{2}^+[631]$	3^-	169(37)	244.4	5.6(2)	5.57(10)
		2^-	218(42)	292.8	5.6(2)	5.80(11)
$\frac{5}{2}^+[642]$	$\frac{5}{2}^+[622]$	5^+	193(60)		3.5(3)	
		0^+	211(63)	230.5	3.5(3)	4.1(1)
$\frac{5}{2}^+[642]$	$\frac{1}{2}^+[631]$	2^+	305(70)	355.7	3.7(3)	3.55(9)
		3^+	372(76)	388.2	3.7(3)	3.83(10)
$\frac{3}{2}^-[521]$	$\frac{5}{2}^+[622]$	4^-	400(100)		5.4(3)	
		1^-	463(110)	400.5	5.4(3)	4.64(11)
$\frac{3}{2}^-[521]$	$\frac{1}{2}^+[631]$	1^-	520(140)		6.0(3)	
$\frac{5}{2}^+[642]$	$\frac{7}{2}^-[743]$	1^-	813(60)		3.6(3)	
$\frac{5}{2}^-[523]$	$\frac{1}{2}^+[620]$	2^-	781(50)	874.1	5.4(4)	5.45(11)
		3^-	867(53)	902.5	5.4(4)	
$\frac{5}{2}^-[523]$	$\frac{1}{2}^-[501]$	3^+	1017(50)	975	5.6(5)	5.0(1)
		2^+	1051(70)	1011	5.6(5)	6.2(1)

TABLE VII. Comparison of observed intensities with intensities predicted by the Alaga rules.

E_i (keV)	I_i^π	K_i	E_f (keV)	I_f^π	K_f	E_γ (keV)	I_γ	I_{Alaga}[a]
230.5	1^+	0						
			44.1	0^-	0	186.4	3277(31)	2307(20)
			75.8	2^-	0	154.7	3595(29)	3665(23)
274.3	1^-	1						
			0.0	1^-	0	274.3	986(10)	995(11)
			44.1	0^-	0	230.2	389(8)	393(4)
			75.8	2^-	0	198.5	138(9)	126(2)
296.4	2^-	1						
			0.0	1^-	0	296.4	203(16)	214(0)
			52.8	3^-	0	243.7	107(7)	80(4)
			75.8	2^-	0	220.6	131(8)	147(6)
372.5	4^-	1						
			52.8	3^-	0	319.8	86(18)	84(16)
			149.8	4^-	0	222.8	49(18)	51(10)

[a]The Alaga branching ratios have been converted to gamma intensities by normalization to the total experimental intensities.

aged rotational parameter of $A(K_>)$ and $A(K_<)$; a is the decoupling parameter for the $\Omega=\frac{1}{2}$ orbital. From our data we have $A=5.69(7)$ keV. Using Eq. (2), we obtain then $|a|=0.99(6)$ to be compared with an average value $a\approx-0.56$ observed for the $\frac{1}{2}^+[631]$ band in the neighboring odd-N ^{241,243}Pu isotopes.[19,27] A similar difference has been observed in ^{244}Am by von Egidy *et al.*[24] The estimated coupling appears to account for only half of the observed moment of inertia difference. Bohr and Mottelson[26] have noted similar effects.

G. The $K^\pi=3^+\{p\frac{5}{2}^+[642]+n\frac{1}{2}^+[631]\}$ band ($BY\uparrow\uparrow$)

An intense 5119.7 keV primary indicates the existence of a probable positive parity level at 418.0(3) keV excitation energy. The low energy data show that this decays by three transitions to levels of the $\{p\frac{5}{2}^-[523]\pm n\frac{1}{2}^+[631]\}$ bands. Assuming that one of the single particles is conserved implies that the initial configuration contains either a $\frac{5}{2}^-[523]$ proton or a $\frac{1}{2}^+[631]$ neutron.

By using the Ritz combination principle, two more levels at 388.17 and 457.16 keV were established. They decay by intraband transitions and again by interband transitions to levels of the $\{p\frac{5}{2}^-[523]\pm n\frac{1}{2}^+[631]\}$ bands. When determined, the latter have $E1$ multipolarities, showing the positive parity character of the initial states. The decay pattern of the lowest observed level indicates $I^\pi=3^+$.

The hypothesis that the K value of the band is 3, consideration of the band head energy and of the rotational parameter, and the probable configuration components noted above, lead us to assign to the band the configuration $\{p\frac{5}{2}^+[642]+n\frac{1}{2}^+[631]\}$. Table VI shows that the band parameters are very close to the values predicted by modeling.

TABLE VIII. Summary of the experimental GM elements and Newby terms obtained for ^{242}Am. They are compared to those obtained in the neighboring nuclei (Ref. 2) and to theoretical values.

Configuration			E_{GM} (keV)			E_N (keV)		
π	ν	Nucleus	Expt.	Theor.[a]	Theor.[b]	Expt.	Theor.[a]	Theor.[b]
$\frac{5}{2}^-[523]$	$\frac{5}{2}^+[622]$	^{242}Am	5.3	96.0	10.0	27.3	−13.8	13.4
		^{238}Np	1.0	95.0	17.0	27.0	−15.2	13.0
		^{240}Am	10.0	96.0	13.0	28.0	−14.7	13.2
		^{244}Am		96.0	7.0	25.4	−14.6	13.0
$\frac{5}{2}^+[642]$	$\frac{5}{2}^+[622]$	^{242}Am				−59.4	−53.6	
$\frac{5}{2}^-[523]$	$\frac{1}{2}^+[631]$	^{242}Am	54.1	61.0	69.0			
		^{238}Np	52.2	60.0	71.0			
		^{244}Am	70.0	61.0	69.0			
$\frac{5}{2}^+[642]$	$\frac{1}{2}^+[631]$	^{242}Am	28.9	63.4	51.0			
		^{238}Np	82.4	70.0	51.0			
$\frac{5}{2}^-[523]$	$\frac{1}{2}^+[620]$	^{242}Am	22.9	116.0	22.0			
$\frac{5}{2}^-[523]$	$\frac{1}{2}^-[501]$	^{242}Am	38.6	44.0	40.0			

[a]Calculation by Boisson *et al.* (Ref. 1).
[b]Calculation by Quentin *et al.* (Ref. 35).

H. The $K^\pi=2^+\{p\frac{5}{2}^+[642]-n\frac{1}{2}^+[631]\}$ band ($BY\uparrow\downarrow$)

An intense 5160.6 keV primary transition populates a level at 377.1 keV (Table I). The $E1$ nature of the 84.12 and 132.56 keV (see Fig. 5) depopulating transitions determines its spin and parity to be 2^+ or 3^+. The decay mode suggests that the initial configuration contains either the $p\frac{5}{2}^-[523]$ or the $n\frac{1}{2}^+[631]$ orbital.

The combination of low energy (n,γ) and (n,e$^-$) results permits us to construct a band having a rotational parameter of 3.55(9) keV. Band head energy and rotational parameter considerations suggest that the configuration is $\{p\frac{5}{2}^+[642]-n\frac{1}{2}^+[631]\}$.

A small difference between the experimental rotational parameter of the $\{p\frac{5}{2}^+[642]\pm n\frac{1}{2}^+[631]\}$ $K^\pi=3^+$ and 2^+ bands is observed (see Table VI). Using Eq. (2), we obtain $|a|=1.23(10)$. This result is similar to that obtained for the $\{p\frac{5}{2}^-[523]\pm n\frac{1}{2}^+[631]\}$ bands and thus confirms a systematic difference between the expected and the observed values of $|a|$ (see Sec. III F). It also supports the configuration assignment. The Gallagher-Moszkowski splitting, 28.9(3.1) keV, will be discussed in Sec. IV B.

I. The $K^\pi=1^-\{p\frac{3}{2}^-[521]-n\frac{5}{2}^+[622]\}$ band ($CZ\uparrow\downarrow$).

A 400.3(4) keV level is populated by a primary transition of 5137.4 keV. It decays (see Fig. 5) to levels of spin 2 and 3 of the $\{p\frac{5}{2}^+[642]-n\frac{5}{2}^+[622]\}$, $\{p\frac{5}{2}^-[523]-n\frac{1}{2}^+[631]\}$, $\{p\frac{5}{2}^-[523]-n\frac{5}{2}^+[622]\}$, and $\{p\frac{5}{2}^-[523]-n\frac{7}{2}^+[624]\}$ bands. The observed multipolarity of the 69.78, 72.81, and 324.84 keV transitions determines that the initial state has negative parity and a spin between 1 and 3. By using the Ritz combination principle, three levels having similar decay patterns are constructed at 419.1, 446.7, and 483.7 keV excitation energy. These are observed to decay to members of the aforementioned bands and also to the ones belonging to the $\{p\frac{5}{2}^+[642]\pm n\frac{1}{2}^+[631]\}K=2$ and 3 bands. From the decay pattern and observed multipolarities, the levels appear to build a negative $K=1$ band, the 400.5 keV level being the band head.

A $K=1$ band at this excitation energy may have, according to the modeling predictions, one of the following configurations: $\{p\frac{3}{2}^-[521]-n\frac{5}{2}^+[622]\}$, $\{p\frac{3}{2}^-[521]-n\frac{1}{2}^+[631]\}$, or $\{p\frac{5}{2}^+[642]-n\frac{7}{2}^-[743]\}$. None of them is based on the proton $\frac{5}{2}^-[523]$ orbital. This is in accordance with the nonobservation of any band level in the neutron transfer reactions.[6] Transitions to final levels where the proton is in the $\frac{5}{2}^-[523]$ orbital imply, therefore, a proton orbital change. We can thus expect that the neutron configuration remains unchanged. The initial neutron is therefore in either the $\frac{5}{2}^+[622]$, the $\frac{1}{2}^+[631]$, or the $\frac{7}{2}^+[624]$ orbital. This selects the possible initial configurations $\{p\frac{3}{2}^-[521]-n\frac{5}{2}^+[622]\}$ or $\{p\frac{3}{2}^-[521]-n\frac{1}{2}^+[631]\}$. The experimental rotational parameter $A=4.64(11)$ keV favors the first alternative (see Table VI).

Problems, however, arise if we consider the decay pattern: levels of the $\{p\frac{3}{2}^-[521]-n\frac{5}{2}^+[622]\}$ band would be expected to decay only to band having either the proton in $\frac{3}{2}^-[521]$ orbital or the neutron in the $\frac{5}{2}^+[622]$ orbital. This does not apply to transitions to levels of the $\{p\frac{5}{2}^-[523]-n\frac{1}{2}^+[631]\}K=2$, $\{p\frac{5}{2}^+[642]\pm n\frac{1}{2}^+[631]\}K=2$ and 3, and $\{p\frac{5}{2}^-[523]-n\frac{7}{2}^+[624]\}K=1$ bands. Von Egidy *et al.*[24] have observed similar decay modes in ^{244}Am. As explanation these authors assume the existence of a mixing of the $\{p\frac{3}{2}^-[521]-n\frac{5}{2}^+[622]\}$ and $\{p\frac{5}{2}^+[642]-n\frac{7}{2}^-[743]\}K^\pi=1^-$ bands. However, this is not possible for parity reasons. We would rather consider a possible mixing of the $\{p\frac{3}{2}^-[521]-n\frac{5}{2}^+[622]\}K=1$ band with the $\{p\frac{3}{2}^-[521]-n\frac{1}{2}^+[631]\}K=1$ and the $\{p\frac{5}{2}^-[523]-n\frac{3}{2}^+[631]\}K=1$ bands. The latter mixing might be related to particle-particle coupling (PCC).[1]

J. The $K^\pi=2^-\{p\frac{5}{2}^-[523]-n\frac{1}{2}^+[620]\}$ band ($AV\uparrow\downarrow$)

The $K^\pi=2^-\{p\frac{5}{2}^-[523]-n\frac{1}{2}^+[620]\}$ band head had been previously observed by Grotdal *et al.*[6] at 873 keV. It appears to be populated by a (n,γ) primary (Table I). Using the Ritz principle, we establish a level with an excitation energy of 874.1 keV which decays by two transitions of 585.2 and 629.6 keV to levels of the $\{p\frac{5}{2}^-[523]+n\frac{1}{2}^+[631]\}$ band. We have developed a band structure with crossover transitions up to spin 5. The experimental band head energy and rotational parameter are in agreement with the predictions (Table VI). All these facts support the band configuration assignment.

K. The $K^\pi=3^-\{p\frac{5}{2}^-[523]+n\frac{1}{2}^+[620]\}$ band ($AV\uparrow\uparrow$)

Only the band head was observed in the transfer reaction[6] at 899 keV. It can be identified as the level at 902.5 keV which we observe to decay by two transitions to levels of the $\{p\frac{5}{2}^-[523]\pm n\frac{1}{2}^+[631]\}$ bands. This decay mode implies the change of the neutron configuration only and thus supports the configuration assignment. The experimental band head energy agrees with the predicted one (see Table VI).

L. Other levels

Three nonassigned levels at 464.4 ($I^\pi=3^-,4^-$), 568.3 ($I^\pi=4^-$), and 612.8 keV ($I^\pi=2^-$) are observed (Fig. 6).

IV. DISCUSSION

A. The g-factors of the ground state band

The g-factors are sensitive to the particle configuration and can thus provide a tool for their identification. As shown by Kern and Struble,[28] we can extract the value of g_R and of a linear combination of g_{Ω_p} and g_{Ω_n} from measurement of a magnetic moment μ and of an intraband branching ratio $\lambda=I_\gamma/I_{\gamma'}$, where γ labels the $I\rightarrow I-2$ and γ' the $I\rightarrow I-1$ transition. In a doubly-odd deformed nucleus, for the special case of a $K=0$ band, the ratio $(G^{KK}/Q_0)^2$ can be evaluated by using the relation (see definition of the symbols in Refs. 28 and 29):

$$\left[\frac{G^{KK}}{Q_0}\right]^2=\frac{1}{2.87\times10^5\times B(\mathrm{I})}\times\frac{(\mathrm{I}-1)^2(\mathrm{I}+1)}{2(2\mathrm{I}-1)}\times\frac{E_\gamma^5}{E_{\gamma'}^3}\times\frac{1}{\lambda}\ . \quad (3)$$

$Q_0(^{242}\mathrm{Am})$ has the value[30,31] $(13.8\pm3.5)b$. For $K=0$ bands $\Omega_p=-\Omega_n$ so that G^{KK} reduces to $G^{KK}=\Omega_p(g_{\Omega_p}-g_{\Omega_n})$, which is independent of g_R. This applies to the ^{242}Am ground state band. Only one branching ratio, for transitions issued from the 149.7 keV 4^- level (Fig. 3), $\lambda=96(24)\times10^{-4}$ is observed. We assumed a relative error of 25% on the intensity of the 73.86 keV transition (Table IV). Using Eq. (3) we obtain $|G^{KK}|=2.98(86)$, so that $|g_{\Omega_p}-g_{\Omega_n}|=1.2(4)$.

This result is larger than the theoretical value calculated by Lamm,[32] i.e., 0.59 if we assume $g_s=0.6g_s^{\mathrm{free}}$. If g_s is decreased to $g_s=0.5g_s^{\mathrm{free}}$, we compute $g_{\Omega_p}-g_{\Omega_n}=0.78$, which is compatible with our result.

A comparison with empirical g factors in odd-A neighbors is not possible; a value $g_{\Omega_p}=0.50(6)$ can be extracted from the published data[33] on ^{237}Np. This differs from Lamm's calculation (0.71 for $g_s=0.6g_s^{\mathrm{free}}$, and 0.78 for $g_s=0.5g_s^{\mathrm{free}}$). ^{237}Pu data on the odd-neutron orbital are not sufficiently precise to extract a meaningful comparison.

The collective g_R factor of the ground state band in ^{242}Am can be computed by use of the relation valid for the case $K=0$:

$$\mu=g_R\times\mathrm{I}\ . \quad (4)$$

The magnetic moment has been measured by Armstrong and Marrus[34] and found to be equal to $\mu=0.388(2)\mu_N$. We thus obtain $g_R=0.388(2)$. This value cannot be compared with model predictions[28] using data in neighboring nuclei since the g_R value of the even core has not been measured.

The above discussion shows that only scarce data on the magnetic properties of actinide nuclei are presently available, so that g factors cannot yet be used for configuration assignments in ^{242}Am.

B. Residual interaction calculations

1. *The Gallagher-Moszkowski splitting*

Several Gallagher-Moszkowski doublets were observed in this work (Table VIII). It is interesting to compare the experimental splittings with the theoretical values calculated by Boisson *et al.*,[1] and by Quentin *et al.*,[35] and also to observation in other doubly-odd neighbors.

Using the theory of residual interaction in doubly-odd nuclei,[36–38] we can write the total energy splitting between the $K^-=|\Omega_p-\Omega_n|$ and the $K^+=\Omega_p+\Omega_n$ states as

$$\Delta E=E_{K^-}-E_{K^+}=\Delta E_{\mathrm{rot}}+\Delta E_{\mathrm{res}}\ , \quad (5)$$

where

$$\Delta E_{\mathrm{rot}}=[A(K^-)\times K^-]-[A(K^+)\times K^+]\ . \quad (6)$$

ΔE_{res} is the Gallagher-Moszkowski splitting.[17] Our experimental results are compared with theoretical values in Table VIII.

Good agreement between the experimental and theoretical values is registered for the $\{p\frac{5}{2}^-[523]\pm n\frac{1}{2}^+[631]\}$ and $\{p\frac{5}{2}^-[523]\pm n\frac{1}{2}^-[501]\}$ configurations.

For the $\{p\frac{5}{2}^-[523]\pm n\frac{5}{2}^+[622]\}$ and $\{p\frac{5}{2}^-[523]\pm n\frac{1}{2}^+[620]\}$ configurations the experimental values are very similar and agree well with those obtained in the recent work of Quentin *et al.*,[35] but they deviate considerably from the values of Boisson *et al.*[1]

An important difference is observed between the experimental values for $\{p\frac{5}{2}^+[642]\pm n\frac{1}{2}^+[631]\}$ configurations in ^{238}Np and ^{242}Am. It has to be noted that in ^{238}Np the two involved bands are the ground state and first excited band for which the data are very precise and reliable.[7] For ^{242}Am, in contrast, the two band heads appear at 355.7 and 388.2 keV, i.e., at excitation energies where the level density is already much larger and where mixing with other band levels is quite probable. The resulting mixings may affect the residual interaction splittings.

2. *Newby shifts*

The Newby shift is defined by Eq. (1). An excellent agreement between experimental and theoretical values is obtained for the $\{p\frac{5}{2}^+[642]-n\frac{5}{2}^+[622]\}$ configuration (see Table VIII). For the $\{p\frac{5}{2}^-[523]-n\frac{5}{2}^+[622]\}$ band, all experimental values are consistent with one another and are closer in value to the calculations of Quentin *et al.*[35] than to those of Boisson *et al.*[1]

C. Statistical cascade calculations

A prediction of the population of a level having a given spin and excitation energy can be obtained by using a statistical model technique described by von Egidy *et al.*[39] In such a model the input parameters are the spin and the parity of the possible capture states $(2^-,3^-)$ and some assumptions on the level density and the hindrance of γ rays compared to the Weisskopf estimates. An accuracy within a factor of about two should be regarded as reasonable. The level density at low energies is estimated from the number of observed levels to be about 50/MeV for Am. In the vicinity of the capture state, the number of levels with spins 2^- and 3^- is[40] $(1.3\pm0.3)\times10^6$/MeV for the compound nucleus ^{242}Am, which gives, with a spin cut-off parameter $\sigma=3$, a total density of 3.3×10^6/MeV. The hindrance factors were chosen so that the total radiation width corresponds[40] to (44 ± 3) meV, the average relative intensity of a single $E1$ transition from the capture state to a low lying level being about 0.05%. For the intensity ratios of $E1$, $M1$, and $E2$ multipolarity transitions, the values $E1{:}M1{:}E2=1{:}0.17{:}0.02$ were taken, as implied by the work of Bollinger and Thomas.[41] These ratios are valid in the rare earth region but were adopted for $A\approx240$ because no other values are available. This corresponds to

TABLE IX. Mean population directly from the capture state of discrete levels in ^{242}Am per 100 neutron captures.

I^π	Number of levels	Experimental mean population	Calculated mean population from capture state 2^-	3^-
0^+	1	0	0	0
0^-	1	0	0.001	0
1^+	1	0.002	0.051	0.000
1^-	3	0.006	0.008	0.001
2^+	2	0.046	0.043	0.042
2^-	4	0.002	0.008	0.008
3^+	5	0.024	0.045	0.043
3^-	8	0.006	0.008	0.008
4^+	3	0.011[a]	0.000	0.042
4^-	5	0.001	0.001	0.007

[a]Unresolved multiplet.

the following partial radiation widths: for a primary $E1$:0.02 meV; $M1$:0.004 meV, and for $E2$:0.0004 meV. These assumptions result in partial transition probabilities of 3×10^{10} s^{-1} for 5.5 MeV $E1$ transitions from the capture state and of 4×10^{7} s^{-1} for 1 MeV $E1$ transitions from the capture state. Results from the calculations on ^{242}Am are given in Table IX, where we compare the mean calculated and experimental direct populations, from the capture state, to the levels below 500 keV excitation energy.

The direct population predictions are sensitive to the capture state spin for the $I=1$ and 4 final level spins. In view of the Porter-Thomas[42] statistical fluctuations, it is not possible to determine clearly the dominance of a spin component in the capture state. The experimental results lie in general between the predicted intensities. In a few cases (see, e.g., level at 364.7 keV) the experimental intensity is significantly larger than the computed one. Such deviations are not unusual (see, e.g., the same analysis[43] for ^{160}Tb).

V. CONCLUSIONS

The present investigation of ^{242}Am involved several complementary thermal neutron capture spectroscopic techniques. It allowed a precise and detailed level scheme to be established. The results of previous studies were confirmed and six new well-developed rotational bands were disclosed. The data obtained were interpreted in the framework of the strong coupling model. The configuration identifications make use of the available spectroscopic information and of modeling predictions[2,7] for the excitation energies and rotational parameters.

We have observed five Gallagher-Moszkowski pairs of singlet and triplet states and extracted the corresponding splittings. Two Newby shifts were also determined. The experimental results are compared to theoretical calculations. The recent theoretical work of Quentin *et al.*,[35] based on a general microscopic approach, appears to reproduce correctly the observed neutron-proton interaction elements. Further systematical studies are needed to test such calculations for a variety of configurations and orbital couplings in order to progress in the understanding of the effective nucleon-nucleon interaction.

ACKNOWLEDGMENTS

The authors wish to thank Prof. T. von Egidy (Munich) for permission to use his program NGAM for the statistical analysis presented in Sec. IV C, to Dr. P. Quentin for communication of the results of his calculations. The excellent cooperation of the reactor and technical staff of the EIR and of the ILL is very much appreciated. This work was supported in part by the Swiss National Science Foundation and under the auspices of the U.S. Department of Energy by the Lawrence Livermore National Laboratory under Contract No. W-7405-Eng-48.

[1]J. P. Boisson, R. Piepenbring, and W. Ogle, Phys. Rev. C **26**, 99 (1976).

[2]R. W. Hoff, J. Kern, R. Piepenbring, and J. P. Boisson, *Capture Gamma-Ray Spectroscopy and Related Topics—1984*, American Institute of Physics Conference, Proceedings Series No. 125, edited by S. Raman (American Institute of Physics, New York, 1985), p. 274.

[3]R. Marrus and J. Winocur, Phys. Rev. **124**, 1904 (1961).

[4]F. Asaro, I. Perlman, J. O. Rasmussen, and S. G. Thompson, Phys. Rev. **120**, 934 (1960).

[5]J. Kantele and O. Tannila, Nucl. Data A **4**, 359 (1968).

[6]T. Grotdal, L. Guldberg, K. Nybo, and T. F. Thorsteinsen, Phys. Scr. **14**, 263 (1976).

[7]V. A. Ionescu, J. Kern, R. F. Casten, W. R. Kane, I. Ahmad, J. Erskine, A. M. Friedman, and K. Katori, Nucl. Phys. **A313**, 283 (1979).

[8]B. Michaud, J. Kern, L. Ribordy, and L. A. Schaller, Helv. Phys. Acta **45**, 93 (1972).

[9]H. H. Schmidt, P. Hungerford, H. Daniel, T. von Egidy, S. A. Kerr, R. Brissot, G. Barreau, H. G. Börner, C. Hofmeyr, and K. P. Lieb, Phys. Rev. C **25**, 2888 (1982).

[10]C. M. Lederer and V. S. Shirley *et al.*, *Table of Isotopes*, 7th

ed. (Wiley, New York, 1978).
[11]A. H. Wapstra and G. Audi, Nucl. Phys. **A432**, 55 (1985).
[12]H. R. Koch, H. G. Börner, J. A. Pinston, W. F. Davidson, J. Faudou, R. Roussille, and O. W. B. Schult, Nucl. Instrum. Methods **175**, 401 (1980).
[13]G. Barreau, H. G. Börner, T. von Egidy, and R. W. Hoff, Z. Phys. A **308**, 209 (1982).
[14]H. G. Börner, W. F. Davidson, J. Blachot, J. A. Pinston, and P. H. M. Van Assche, Nucl. Instrum. Methods **164**, 579 (1979).
[15]W. Mampe, K. Schreckenbach, P. Jeuch, B. P. K. Maier, F. Braumandl, T. Larysz, and T. von Egidy, Nucl. Instrum. Methods **154**, 127 (1978).
[16]R. S. Hager and E. C. Seltzer, Nucl. Data Table A **4**, 1 (1968).
[17]C. J. Gallagher, Jr. and S. A. Moszkowski, Phys. Rev. **111**, 1282 (1958).
[18]N. D. Newby, Phys. Rev. **125**, 2063 (1962).
[19]Y. A. Ellis-Akovali, Nucl. Data Sheets **44**, 407 (1985).
[20]Y. A. Ellis-Akovali, Nucl. Data Sheets **33**, 79 (1981).
[21]G. Alaga, K. Alder, A. Bohr, and B. R. Mottelson, K. Dan. Vidensk. Selsk. Mat.-Fys. Medd. **29**, No. 9 (1955).
[22]M. R. Schmorak, Nucl. Data Sheets **40**, 1 (1983).
[23]Y. A. Ellis-Akovali, Nucl. Data Sheets **33**, 119 (1981).
[24]T. von Egidy, R. W. Hoff, R. W. Lougheed, D. H. White, H. G. Börner, K. Schreckenbach, D. D. Warner, and P. Hungerford, Phys. Rev. C **29**, 1243 (1984).
[25]T. H. Braid, R. R. Chasman, J. R. Erskine, and A. M. Friedman, Phys. Rev. C **4**, 247 (1971).
[26]A. Bohr and B. R. Mottelson, *Nuclear Structure* (Benjamin, New York, 1975), Vol. II, p. 122.
[27]R. R. Chasman, I. Ahmad, A. M. Friedman, and J. R. Erskine, Rev. Mod. Phys. **49**, 833 (1977).
[28]J. Kern and G. L. Struble, Nucl. Phys. **A286**, 371 (1977).
[29]F. Boehm, G. Goldring, G. B. Hagemann, G. D. Symons, and A. Tveter, Phys. Lett. **22**, 627 (1966).
[30]K. E. G. Löbner, M. Vetter, and V. Hönig, Nucl. Data Table **A7**, 495 (1970).
[31]E. N. Shurshikov, M. L. Filchenkov, Yu. F. Jaborov, and A. I. Khovanovich, Nucl. Data Sheets **45**, 509 (1985).
[32]I. L. Lamm, Nucl. Phys. **A125**, 504 (1969).
[33]Y. A. Ellis-Akovali, Nucl. Data Sheets **49**, 181 (1986).
[34]L. Armstrong and R. Marrus, Phys. Rev. **144**, 994 (1966).
[35]P. Quentin, L. Bennour, J. Libert, M.-G. Porquet, D. E. Medjadi, and M. Meyer, 6th Capture Gamma-Ray Symposium, Leuven, Belgium, 1987 (Institute of Physics, London, in press).
[36]N. J. Pyatov, Izv. Akad. Nauk SSSR **27**, 1436 (1963).
[37]N. J. Pyatov and A. S. Chernyshev, Izv. Akad. Nauk SSSR **28**, 1073 (964).
[38]H. D. Jones, N. Onichi, T. Hess, and R. K. Sheline, Phys. Rev. C **3**, 529 (1971).
[39]T. von Edigy, *Neutron Capture γ-Ray Spectroscopy* (IAEA, Vienna, 1969), p. 541.
[40]J. E. Lynn, *The Theory of Neutron Resonance Reactions* (Clarendon Press, Oxford, 1968).
[41]L. M. Bollinger and G. E. Thomas, Phys. Rev. C **2**, 1951 (1970).
[42]C. S. Porter and R. G. Thomas, Phys. Rev. **104**, 483 (1956).
[43]J. Kern, G. Mauron, B. Michaud, K. Schreckenbach, T. von Egidy, W. Mampe, H. R. Koch, H. A. Baader, D. Breitig, U. Gruber, B. P. K. Maier, O. W. B. Schult, J. T. Larsen, R. G. Lanier, J. J. Tambergs, and M. K. Balodis, Nucl. Phys. **A221**, 333 (1974).
[44]J.-L. Salicio, S. Drissi, J. Kern, G. G. Colvin, and K. Schreckenbach, University of Fribourg, Institute of Physics Report No. IPF-PAN-1, 1987 (unpublished).